2 Fusion Plasma Physics

Work in fusion plasma physics includes 14 physics tasks and 3 IFE "keep-in-touch" activity tasks. The tasks are grouped under the four following sub-headings:

- Energy and particle confinement and transport
 - Tokamak modelling
 - o Integration of transport and MHD codes at JET (ITC) (EFDA JET Task)
 - Studies of material erosion and re-deposition on plasma-facing components from the TEXTOR tokamak
- Fusion plasma diagnostics
 - Spectrometry of soft X-ray emission from W7-X stellarator by the use of fast counting semiconductor detectors
 - Application of semiconductor detectors to measurement of X-ray radiation from tokamak (MAST)
 - Čerenkov detectors for fast electron measurements: new diagnostics for Tore-Supra
 - Development and application of neutron diagnostics for magnetic confinement devices (JET and W7-X)
 - Applications of solid-state nuclear track detectors (SSNTDs) for fast ion and fusion reaction product measurements in TEXTOR experiments
 - o C-, O- monitor system for W7-X
 - o Microwave diagnostic development
 - Detection of the delayed neutrons from activation of fissionable materials in the neutron field at fusion-plasma devices
- Development of concept improvements: theory and modeling development for improved concepts
 - o Stellarator (3D fluid) modelling for W-7X and TEXTOR-DED
 - Nonlinear dynamics of fast ion driven plasma modes near instability threshold theoretical basis for integrated tokamak modeling
 - Numerical analysis and evaluation of the structural mechanical behaviour of central support connections under electromagnetic forces for W7-X
- Inertial fusion energy "keep-in-touch" activity
 - o Investigation of influence of nonthermal phenomena on energy transfer in IFE
 - o Studies on fast ignition of inertial fusion using laser-driven proton beams
 - o Formation of plasma jets and their interaction with ambient media

2.1 Tokamak modelling

Roman Zagórski Institute of Plasma Physics and Laser Microfusion zagorski@ifpilm.waw.pl

Sebastian Głowacz, and Roman Stankiewicz

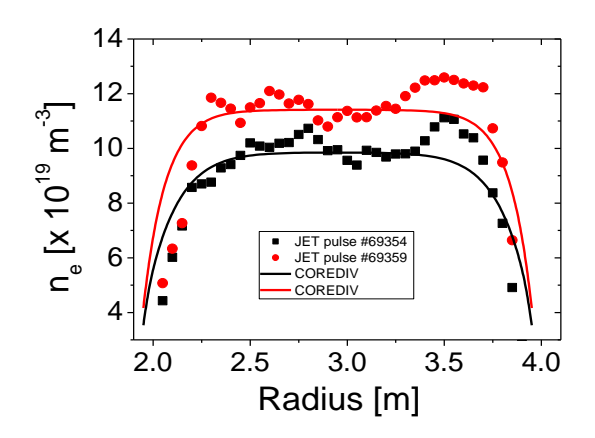
Abstract

FULL TEXT

The work done in 2007 has been concentrated on global simulations of plasma parameters in tokamaks. In particular, we have investigated the role of core—edge coupling and the plasma-wall interactions on the tokamak performance. Simulations have been done for present day tokamaks (JET, FTU, COMPASS-D) as well as for future devices (ITER, DEMO, FAST). The basic numerical tool which has been used for our studies is the COREDIV code which is able to describe self-consistently the core and boundary plasma regions in tokamaks. The code has been successfully applied to the JET and FTU tokamak plasmas and very good agreement with experimental data has been found. Apart of recovering the global plasma parameters, the code reproduces also plasma profiles as well as the interplay (exchange mechanism) between seeded and intrinsic impurities. Since the benchmark exercise of the COREDIV code with the experimental data was successful, the code has been applied to systematic studies of future devices. It has been used to estimate discharge parameters, in particular the heat load to the divertor plates, in the FAST (FT3) tokamak as well as in ITER and DEMO reactors.

Summary

The work done in 2007 has been concentrated on global simulations of plasma parameters in tokamaks. In particular, we have investigated the role of core –edge coupling and the plasma-wall interactions in the determining discharge parameters. Simulations have been done for present day tokamaks (JET, FTU, COMPASS-D) as well as for future devices (ITER, DEMO, FAST). The basic numerical tool which has been used for our studies is the COREDIV code which is able to describe self-consistently the core and boundary plasma regions in tokamaks. The code has been successfully applied to the JET and FTU tokamak plasmas and very good agreement with experimental data has been found (in Figs. 1-2 we shown example of benchmarking exercise made for JET plasmas).



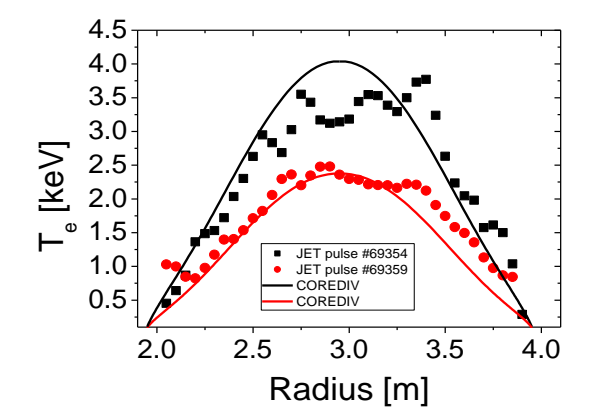


Figure 1 Comparison of experimental and numerical profiles of the plasma density for JET shots #69354 ($P_{aux} = 23$ MW, $n_e = 9.4 \times 10^{19} \, \text{m}^{-3}$) and #69359 ($P_{aux} = 17$ MW, $n_e = 10.2 \times 10^{19} \, \text{m}^{-3}$)

Figure 2 Comparison of experimental and numerical profiles of the plasma temperature for JET shots #69354 ($P_{aux} = 23$ MW, $n_e = 9.4 \times 10^{19}$ m⁻³) and #69359 ($P_{aux} = 17$ MW, $n_e = 10.2 \times 10^{19}$ m⁻³)

In addition to recovering the global discharge parameters, such as temperature and density profiles, total radiated power, Z_{eff} , the interplay between seeded nitrogen and intrinsic carbon is also reproduced [2]. Predictions for the JET discharges with higher plasma current $I_p = 3.5$ MA and different input

powers ($14 < P_{aux} < 23$ MW) demonstrate that it is possible to achieve high radiation fractions (> 80%) and simultaneously reduce both the plasma collisionality and Z_{eff} . Indeed, the moderate confinement characteristic for the type III ELMy discharges allows for high radiation levels with low impurity concentration in the core.

Since the benchmarking of the COREDIV code with the experimental data was successful, the code has been applied to systematic studies of future devices. It has been used to estimate discharge parameters, in particular the heat load to the divertor plates, in the FAST (FT3) tokamak as well as in ITER and DEMO reactors.

We have simulated impurity seeded ITER discharges with two different target plate materials: carbon and molybdenum. The relatively weak decrease of the amplification factor Q with increasing the confinement of the He ash is a direct consequence of the computed reduced release of intrinsic impurities in the presence of helium. This result allows the viability of a high density, radiative divertor to be considered as a realistic option, limiting the concern of helium pumping.

In the case of a Mo target, for the ITER inductive reference scenario with medium density/high confinement the power to the plate becomes acceptably low only at high values of Ar/Ne puffing rate, with Mo concentration below 10⁻⁴ % and with the radiative properties of the discharge fully dominated by the injected impurities. In such a situation the discharge may easily become radiatively unstable. On top of that, the power through the separatrix decreases rapidly at high puffing rates, with possible related implications for the L-H mode threshold. In the case of C plate, Ar puffing appear to be appropriate choices to reduce significantly the power load to the plate in fully integrated edge-core scenarios.

The combine effect of seeded and sputtered impurities on the power load density and on the fusion reactivity of the demo reactors (DemoA and DemoD) has been also investigated. Steady state operation parameters of thereactor have been found numerically for different gas puff level of injected impurity (Ar) for H-mode confinement regime. Molybdenum and Tungsten have been considered as the plate materials. The contributions of main ions and impurities to plate materials sputtering have been taken into account. The results of numerical modelling with COREDIV code show that it might to problematic to reduce the heat load to acceptable level. The reduction of the power flux due to increase of the seeded impurity density leads to decrease of sputtered impurity density and is paid for by decrease of the alpha power (amplification factor Q). It has been found that up to 60 to 80 % of the alpha power can be radiated, however this might be insufficient for the reactor DemoA.

Conclusions

The work done in 2007 has been focused on simulations of plasma parameters in tokamaks. Apart of applying of the EDGE2D code to the analysies of the boundary plasma parameters in the impurity seeded JET discharges, we have mostly concentrated on global simulations of tokamk plasmas with the COREDIV code. The code is able to couple self-consistently the core and edge plasma in tokamaks and thus it is a very good tool to assess the influence of seeded and intrinsic impurities on heat load to the target plates, in particular in fusion reactors. The code has been successfully benchmarked against the experimental data from JET and FTU tokamaks and applied to investigations of future devices like ITER, DEMO, FAST.

Collaboration

Association EURATOM – ENEA, Energy Research Center, Frascati, Italy

Association EURATOM - FZJ, Institute of Plasma Physics, Juelich, Germany

Association EURATOM – CEA, Cadarache, France

Association EURATOM – Belgium State, Royale Military Academy (ERM/KMS), Brussels

Association EURATOM – VR Alfven Laboratory, Royal Institute of Technology, Sweden

Association EURATOM - UKAEA Culham Science Center, Abingdon, UK

- [1] J. Rapp, et al., Nuclear. Fusion, 44 (2004) 312
- [2] J. Rapp, et al., J. Nuclear Materials, 337-339 (2005) 826
- [3] G. Telesca et al., Nucl. Fusion,40 (2000) 1845
- [4] R. Zagórski and R. Stankiewicz, J. Nuclear Materials, 313-316 (2003) 899
- [5] R. Pánek, O. Bilyková, V. Fuchs et al., Czech. J. Phys. 56, Suppl. B, B125 (2006)
- [6] J. Rapp et al., J. Nuclear Materials, 337-339 (2005) 826
- [7] R. Simonini et al., Contrib. Plasma Phys. 34, 368 (1994)
- [8] R. Stankiewicz and R. Zagórski, J. Nucl. Mater. 337-339 (2005) 191

2.2 Integration of Transport and MHD Codes at JET (ITC)

Roman Zagórski Institute of Plasma Physics and Laser Microfusion zagorski@ifpilm.waw.pl

Abstract

A new model for drifts and self-consistent electric field has been implemented to the Edge2D code in the frame of the ITC project. Numerical tests were made for pure hydrogenic plasmas in the SOL, which showed improved robustness and consistency.

Summary

The Project "Integration of Transport and MHD codes at JET (ITMC)" was launched in the beginning of 2004 with the main objective to bring all JET-based 1.5D core transport codes, linear MHD and drift turbulence stability codes, under the same user-friendly environment. All codes should share the same I/O files as well as catalogue management system. The main advantage of such a unified approach (in addition to its user-friendliness) is that it allows easy code benchmarking. Taking account of the fact that different codes were optimised to study different phenomenon, this benchmarking could lead to a fast progress in both code development and predictive modelling.

During 2004, the Project "Integration of Transport and MHD Stability Codes at JET" has led to the creation of a common user-friendly environment for many transport and MHD stability codes at JET, which allows direct code comparisons and code benchmarking.

Further progress in code integration is driven by two main needs:

- I. Code benchmarking and model validation
- II. Incorporation of new modules into JAMS

It is important to note that the successful integration of transport and MHD codes at JET has led to the creation of a unique suite of codes, which can be used from any EU Association. It has attracted many new users and this has increased significantly the workload required for code maintenance and upgrade. It is also worth noting that both transport and MHD codes rely more and more on highly specialised models, which can only be maintained properly by their creators. Therefore, the Tasks for 2006 included a significant activity related to code and model upgrade and benchmarking.

The contribution of IPPLM to the project consisted in the Task 9: Improvements to the implementation of drifts in EDGE2D and the corresponding work was done in January 2007.

The Task was to improve the drift model implementation in EDGE2D. In the original drift model, the calculation of the self-consistent plasma potential inside the separatrix was rather crude, and prone to numerical problems. In addition, it was found that the way the drift fluxes were separated into components could give rise to numerical artefacts due to inaccurate cancellation of compensating components. The task therefore required a complete replacement of the drift model with a more rigorous implementation due to R. Zagórski (IPP-Poland), which is detailed in Annex 11 of the Final ITC Project Report [1], and a careful numerical implementation to ensure the exact cancellation drift flux components where required. This drift model was fully implemented and preliminary tests were made for pure hydrogenic plasmas in the SOL, which showed improved robustness and consistency.

Conclusions

The new model for drifts and self-consistent electric field has been implemented to the Edge2D code. Calculations have been performed to test the performance of the new module for a range of plasma parameters. It appeared that the new model gives very similar results as the old Radford model, at least for cases for which the comparison was possible (the Radford's model did not converge for all considered situations). In addition, the simulated conditions correspond to the test cases already done

by the B2 code and they constitute a part of the benchmarking exercise of both codes (Edge2D and B2).

Collaboration

Association EURATOM - UKAEA, Culham Science Center, UK

References

[1] Final report on the Project "Integration of Transport and MHD Codes at JET" (ITMC) as part of 2006-2007 JET Workprogramme

2.3 Studies of material erosion and re-deposition on plasma facing components from the TEXTOR tokamak

Elżbieta Fortuna

Warsaw University of Technology, Materials Science and Engineering Faculty elaf@inmat.pw.edu.pl

Marek Psoda, Witold Zieliński, Mariusz Andrzejczuk, Marcin Pisarek, Tomasz Płociński, Stanisław Szpilewicz, and Krzysztof J. Kurzydłowski

Abstract

To improve understanding of the mechanisms of material erosion and re-deposition, studies of the microstructure and chemical composition of the plasma facing components originating from the TEXTOR and ASDEX-Upgrade tokamaks were carried out. The following investigations were undertaken:

- 1. characterization of the plasma-induced damage in high Z metals used as limiters,
- 2. characterization of material mixing occurring in high Z metals used as limiters,
- 3. characterization of the co-deposits.

Summary

To improve the understanding of the mechanisms of material erosion and re-deposition, studies of the microstructure and chemical composition of the plasma facing components originating from the TEXTOR and ASDEX-Upgrade tokamaks were carried out. In particular the following tasks were completed:

- 1. XRD studies of material mixing on Plasma Facing Components from TEXTOR tokamak and
- 2. Post mortem analysis of tungsten coated strike point tile from the upper inner divertor of ASDEX-Upgrade.

Ad. 1.

The study was carried out for two tungsten limiters exposed to plasma at TEXTOR: (a) a castellated block of mushroom shape and (b) a vacuum plasma sprayed (VPS) thick coating on graphite limiter block. In the case of castellated limiter block, the deposits formed in the poloidal gaps were investigated. The XRD analysis revealed tungsten oxide WO_2 and cooper in the deposit (Fig. 1). To the best knowledge of the authors the presence of W-oxide on components retrieved from a tokamak has not been reported earlier in the literature. One can conclude that the enhanced material migration and mixing should be taken into account if the oxygen assisted fuel removal techniques are applied in next step devices

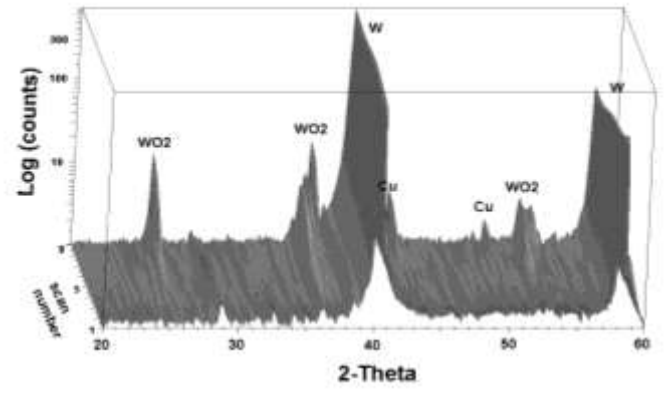


Figure 1 Distribution of WO₂ and Cu across deposit

For tungsten coated graphite limiter, the XRD measurements were performed at two sides of the block (in the gap between the two limiter stones as well as at the outer surface), for three different positions.

The deposit representative XRD spectrum is shown in Fig. 2. The tungsten carbide, WC, is the main tungsten phase on the graphite background. Minor peaks were identified as originating from tungsten subcarbide W_2C and elemental tungsten. The results are representative for both faces. It should be noted that graphite crystal lattice parameter is distorted by presence of C-D species in the co-deposit. If intense carbon-tungsten mixing leading to carbide formation occurs on a large scale in carbon- and tungsten- containing environments, brittle carbides on PFCs are formed.

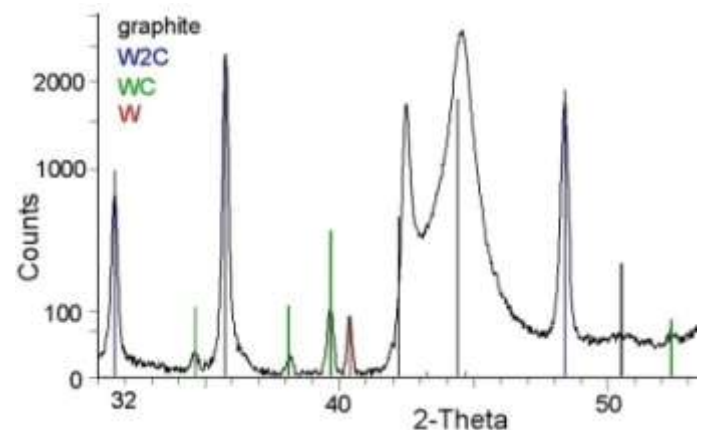
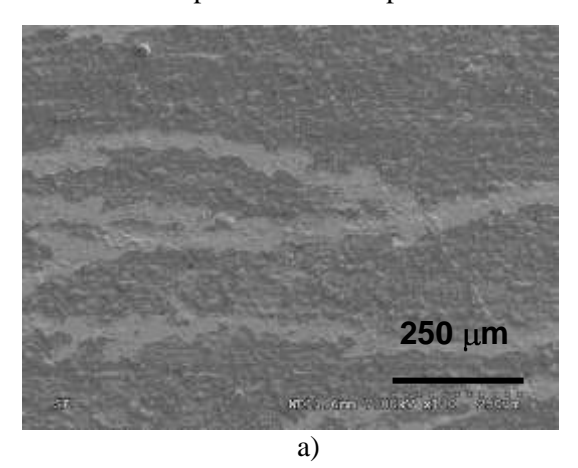


Figure 2 Diffraction pattern of deposit present at the side surface of tungsten coated graphite limiter block **Ad. 2**

A PVD tungsten coated strike point tile from the upper inner divertor region, which was installed in the tokamak ASDEX Upgrade for several campaigns until 2006, was studied. The aim of post-mortem analyses was material mixing, a new compound formation and quest for evidence of plasma-induced damage of the tungsten coating. The coating morphology was modified by high-heat loads and codeposition of impurity species from the plasma. Comprehensive analysis carried out by XPS, TEM, XRD, HRSEM revealed: (i) mixed B-O-C film formation (below 100 nm), (ii) local tungsten layer melting,

(iii) strongly textured columnar character of PVD tungsten layer (3 to 4 micron thick). No evidence of carbide formation at tile/coating side was found.

The co-deposit contained fuel species as well as carbon (41at.%), boron (23at.%) and oxygen (30at.%). Nitrogen was present at the level of 3at.% and tungsten below 1at.%. XPS analysis showed that boron was present in the deposit in the elemental form, in the form of oxides and oxy-nitrides.



50 μmb)

Figure 3 SEM images of tile surface

Collaboration

Association EURATOM – VR, Alfvén Laboratory, KTH, Stockholm, Sweden Association EURATOM – FZJ, Institute of Plasma Physics, Juelich, Germany Association EURATOM – IPP, Garching, Germany

2.4 Spectroscopy of soft x-ray emission from the W7-X stellerator (pulse height analysis –PHA and multi-foil spectroscopy – MFS)

Leszek Ryć Institute of Plasma Physics and Laser Microfusion (IPPLM) ryc@ifpilm.waw.pl

Sławomir Jabłoński, Jerzy Wołowski, Jacek Kaczmarczyk, Agata Czarnecka, and Monika Kubkowska

Abstract

An experimental PHA system, which will be used for testing different arrangements of the x-ray spectroscopy system, is completed at IPPLM, Warsaw. The spectrometry apparatus is based on the use of a silicon drift detector from the firm Amptek, USA. Alternatively, special detectors based on wide-band-gap materials, which are assumed to be suitable for the PHA system used at intense neutron emission, are being developed. The code *IONEQ* for predicting x-ray emission from plasma, which were developed and installed at IPP Greifswald, was made accessible in IPPLM and is used remotely for designing the PHA and MFS systems. A similar code *RAYX* was developed in IPPLM, which has an option of evaluation of x-ray and neutron response of semiconductor detectors.

Summary

A pulse height analysis (PHA) diagnostic system is planned to be used on W7-X stellarator to obtain the shape of x-ray spectrum. It will be used for determining the electron temperature of plasma and ionic content of a plasma, as well as for observing non-thermal effects by the measurement of the hard x-ray component and for identifying impurities. The diagnostics is based on the application of a semiconductor detector. An experimental PHA system is completed at IPPLM. It is designed for testing detectors and other components of the spectrometry systems, optimisation of the system for the best spectral resolution, and testing different configuration and options of the system (different geometry, the solutions of using a detector in vacuum, etc.).

A modern solution for the PHA spectrometry system which must operates at high counting rate is the application is the use of a Si drift detector [1] which is of very low capacitance and thus predestined for obtaining a good spectral resolution at high counting rate and also at moderate cooling (-20 °C). To assure fairly high energy resolution at high counting rate, a digital processing system (DSP) is used for processing the data from the drift detector. The USA firm Amptek was chosen for purchasing the needed apparatus for the experimental PHA system. This firm was ready to deliver individual components or modules of the system separately that gave the possibility of experimenting with different configuration which would be useful for application in the environment of the stellarator.

Some work has been started on developing substituting detectors which can replace the Si drift detector at some special experimental conditions - high temperature or intense neutron emission. This subject is dealt within the range of collaboration between Institute of Electrical Engineering, Slovak Academy of Sciences, Association EURATOM, Bratislava and IPPLM. The main subject of the collaboration is development of new detectors based on wide-band high-Z semiconductor materials (e.g., GaAs) which could be resistant to neutron damaging [2].

For designing a PHA system and also for assuring its proper operation (e.g., avoiding overloading) it is important to know the intensity of the measured x-ray radiation. The code *IONEQ* [3] developed and installed at IPP Greifswald was made accessible in IPPLM and is used remotely for designing the PHA system. A somewhat different code *RAYX* for evaluation of x-ray emission for only free-free and free-bound x-ray radiation was developed in IPPLM which has an option for evaluation of the response of a semiconductor detector or an array of them to x-rays that can be useful for designing both, the PHA and MFS systems. Moreover, the code delivers the data about x-ray and also neutron emission, that is useful for the evaluation of the possible disfiguring effects in detector.

Conclusions

All the milestones which were specified in the Work Programme for 2007 have been realized, namely:

- completion of the experimental spectrometry system at the IPPLM
- developing the numerical codes for optimisation of filters and detectors for the MFS system as well as for deconvolution of X-ray spectrum
- developing concepts of the PHA and MFS systems

The project is realised as a result of collaboration of three sides: IPP Greifswald, IEE Bratislawa and IPPLM Warsaw. A completion of an experimental PHA system at IPPLM is realised. The spectrometry apparatus based on the use of a silicon drift detector was ordered in the firm Amptek, USA. Some works for recognition of the most suitable detectors made from GaAs for the PHA system were initiated. The knowledge obtained from the first experiments and also the results obtained with the use of simulation codes should deliver all needed information for designing and fabrication of the final version of the PHA system which will be used at W7-X.

Collaboration

Association EURATOM – IPP, Greifswald, Germany Association EURATOM – SA Institute of Electrical Engineering, Bratislava, Slovakia

- [1] E. Gatti, P. Rehak, "Review of semiconductor drift detectors", Nucl. Inst. and Meth. in Phys Res. A 541 (2005) 47-60.
- [2] F. Dubecký, P. Boháček, B. Zaťko, T. Lalinský, Š. Chromík, M. Ladzianský, V. Nečas, L. Ryć, and A. Weller, "Performance study of bulk semi-insulating GaAs radiation detectors: Role of ohmic contact metallization", accepted for 9th International Conference on Applications of Nuclear Techniques (ANT08), Crete, Greece 8-14 June 2008.
- [3] Code IONEQ for simulation of X-ray emission, A. Weller, IPP Greifswald, personal communication.

2.5 Measurement of X-ray emission from tokamak (MAST) plasma by the use of matrix detectors

Leszek Ryć Institute of Plasma Physics and Laser Microfusion ryc@ifpilm.waw.pl

Sławomir Jabłoński, Jacek Rzadkiewicz, Jerzy Wołowski, Agata Czarnecka, and Jacek Kaczmarczyk

Abstract

A design of the multicolour 1D soft x-ray imaging system for future experiments at the Mega-Amper Spherical Tokamak (MAST) and results of the numerical simulations of operation of the system based on initial assumptions about the state of the tokamak plasma as well as the parameters and geometry of the detection system are presented. In simulations, the operation of an array of semiconductor detectors is compared with the operation of an array of scintillator-photomultiplier combination.

Summary

The operation of the multicolour soft x-ray (SXR) imaging system that is going to be applied on MAST is based on filter absorption technique. The system consists of a set of arrays of detectors, pinholes and filters attached to each array, together with suitable readout electronics, see Fig.1. The signals from the detectors are transferred to preamplifiers in the case of semiconductor detectors and to a multi-channel photomultiplier by fibre optics connections and further also to preamplifiers in the case of scintillator detectors.

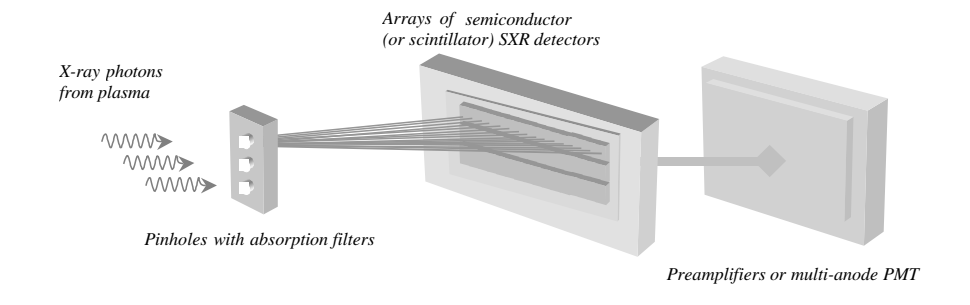


Figure 1. The SXR 'multi-colour' array system planned for MAST.

The imaging system is expected to provide T_e continuous profile measurements with high time resolution (about 10 µs) and relatively high spatial resolution (~1 cm). In this work comparison simulations for application of both silicon detectors and scintillators based measurement systems dedicated for MAST SXR diagnostics were made [1]. The simulations were carried out with the use of a specially developed computer code RAYX. In the evaluations, it was assumed that the radiation is dominated by the continuous component and the line radiation can be discriminated by using filters and therefore neglected at the first approximation. The code *RAYX* simulates the composition of ionic stages and intensity of f-f and f-b radiation coming from inelastic electron-ion collisions for various parameters of plasma. Basing on input assumptions about the configuration of the detection system and the amount of impurities, the code predicts the response of the 1D imaging system for a given plasma density and temperature spatial profiles.

The numerical simulations were performed for the MAST tokamak facility geometry (Fig. 2) where inner and outer plasma radiuses are r = 20 cm and R = 145 cm, respectively.

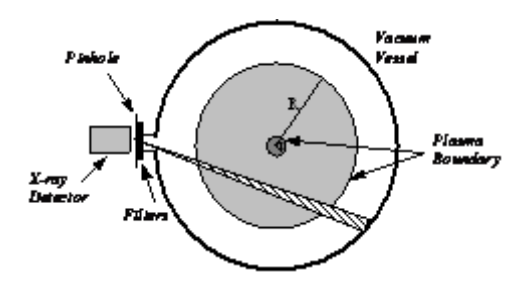
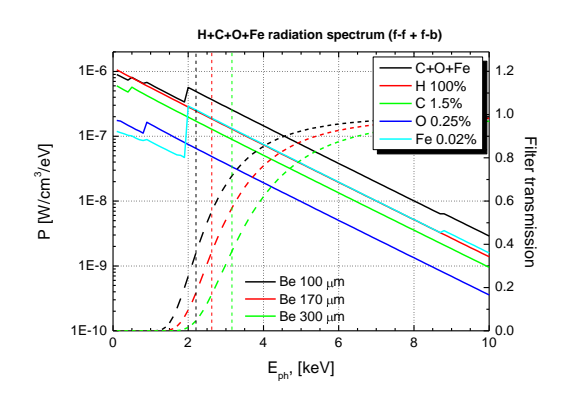


Figure 2. Plasma geometry of the measurement on MAST used in the RAYX code.

It is assumed that all detectors (of pixel size of $\sim 2.8 \times 2.8$ mm) are thick enough to cover photon energies from 0.1 to 10 keV. The three detector arrays are filtered by 100, 170 and 300-um Be filters. The filters should discriminate the line radiation emitted by C, O and Fe impurities up to 1.3 keV. The computer code calculates the current produced in a pixel of the Si array (or the current generated from the photocathode of one channel of the multianode photomultiplier) by x-rays coming from the chord area viewed by the pixel.

Figure 3 presents the simulations of the chord-averaged x-ray spectral power viewed from the central pixel. The radiation comes mostly from the Fe impurity. Figure 4 presents simulations of the currents from the array filtered with a 170-µm Be filter and measured with the use of the Si and CsI(Na) detector arrays directly from a Si pixel, or a photocathode of a single photomultiplier channel.



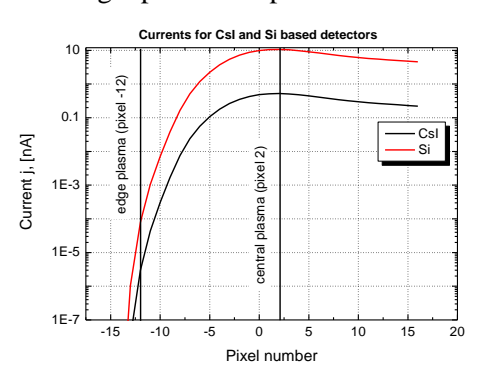


Figure 3. Chord-averaged x-ray spectral power viewed Figure 4. Simulation of total current from Si and from the central pixel in function of photon energy for CsI(Na) detector arrays in function of a pixel plasma with parameters specified in Fig. 2: H 100% - number, evaluated for 170-µm Be filter and reference plasma without impurities, C+O+Fe - plasma impurities: 0.02 % Fe, 0.25% O and 1.5% C. from impurities alone; contribution from individual impurities are shown separately.

The predicted values of the currents obtained from the RAYX code seen from the Si detection system are in the range of 0.01 pA - 10 nA therefore the measuring system in this configuration does not look promising for the application as it would need using an unhandy, very sensitive and noiseless amplifiers. The currents seen from the photocathodes are even smaller (1fA-1nA) but they can be easily amplified inside the photomultiplier by a factor even up to 10⁶ so the reasonable currents are produced.

Summary

A multicolour SXR diagnostic system which is based on the use of filter absorption technique is planned to be applied on MAST. It consists of a set of arrays of detectors, pinholes and filters attached to each array, together with suitable readout electronics. It could be based on silicon or scintillator xray array detectors. In this work we present comparison simulations for application of both types of detectors. The simulations were carried out with the use of a specially developed computer code RAYX. Only bremsstrahlung and recombination radiation were taken into consideration in this analysis. The application of a semiconductor arrays occurs to be not promising whereas the application of scintillation detector assures a proper operation of the measuring system.

Conclusions

All the milestones concerned on the development of the code *RAYX* and its use in assessment of operation of the 1-D imaging system on MAST have been realized.

The predicted values of the currents obtained from the RAYX code seen from the Si detection system are so small (less than 10 nA) that the measuring system in this configuration does not look promising for the application. The measuring system based on a photomultiplier is promising for the application assuming that low-noise amplifiers will be added to each anode of the photomultiplier.

Collaboration

Association EURATOM – UKAEA, Culham Science Centre, Abingdon, UK

References

[1] S. Jabłoński, A. Czarnecka, J. Kaczmarczyk, L. Ryć, J. Rzadkiewicz, "Assessment of a 1-D Multicolour X-ray Imaging System for the MAST ST", Conference PLASMA'2007, Greifswald, 16-19 October 2007

2.6 Cherenkov detectors for fast electron measurements: new diagnostics for Tore-Supra

Lech Jakubowski
The Andrzej Sołtan Institute for Nuclear Studies
jakubowski@ipj.gov.pl

Marek J. Sadowski, Krzysztof Czaus, Karol Malinowski, Marek Rabiński, Jacek Stanisławski, Jarosław Żebrowski, Marcin Jakubowski, Paweł Karpiński, and Andrzej Wiraszka

Abstract

The detailed analysis of problems connected with measurements of fast electron beams within the TORE-SUPRA facility at CEA-Cadarache, which was performed by the IPJ team in the previous years, made possible to design an appropriate Cherenkov-type detector. In 2007 further progress in the design and manufacturing of such a detector, which might enable electron measurements under extremely difficult thermal conditions, was achieved at IPJ. On the basis of that analysis there were also elaborated simpler Cherenkov detectors, designed for studies of electron beams inside tokamaks producing lower thermal loads upon measuring heads. Those detectors have already been used for experiments within CASTOR device in Prague and ISTTOK facility in Lisbon.

Summary

In 2007 research on design and applications of Cherenkov-type detectors for measurements of fast electrons in tokamak-type facilities were concentrated mainly on 3 different tasks:

- a) Continuation of the manufacturing of a new Cherenkov-detector prototype designed especially for studies of supra-thermal electrons within TORE-SUPRA facility in CEA-Cadarache;
- b) Analysis of experimental results obtained within CASTOR device in the previous year and the elaboration of papers for publication;
- c) Manufacturing and preparation of the simplified Cherenkov detector for measurements in ISTTOK facility in IST-Lisbon.

Ad a). The manufacturing of different parts of a prototype Cherenkov-detector, as designed especially for experiments within TORE-SUPRA facility in CEA-Cadarache, was continued. New diamond radiators were bought and prepared for the coating with Mo-layers. Connections of radiators and optical-fibers were discussed and agreed with our French partners. The described construction and appropriate selection of constructional materials ensure an effective transfer of heat deposited upon the Cherenkov-probe surface. In order to reduce the thermal load the French team at CEA-Cadarache designed a special mobile shaft, which will enable the Cherenkov-probe to be exposed for short periods only, but several times during a single discharge. This shaft should be ready in the first quarter of 2008.

Ad b). This report presents results obtained from the last experimental campaign, which was performed with the use of an improved version of the Cherenkov detector within CASTOR facility in IPP-Prague. Some examples of the time-resolved electron signals, which were recorded in CASTOR discharges with high- and low-density plasma, are presented in Fig.1.

From an analysis of the collected experimental results it was possible to deduce about the behavior of fast electron beams inside CASTOR. In particular it was possible to determine a dependence of electron beams intensity on the radial position of the Cherenkov detector for discharges of different plasma densities. It was found that the character of the recorded electron signals depended very strongly on the density of plasma as well as on the radial distance of the measuring Cherenkov detector from the tokamak chamber axis. With an increase in the distance from that axis the electron

signals decreased and they appeared later. The results, which were obtained at the discharge current equal to about 10.5 kA and two different values of the plasma density, are shown in Fig. 2.

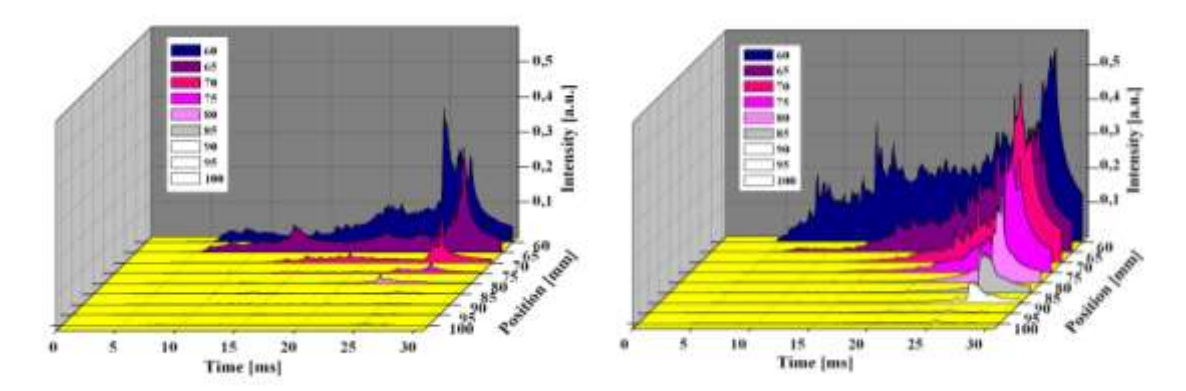


Figure 1 Temporal changes of the electron signals as a function of the position of the Cherenkov detector along the CASTOR minor radius, as observed for high-density discharges (on the left) and low-density discharges (on the right)

The presented diagram shows the time-integrated values of the recorded electron signals proportional to the fast electron streams, which reached the Cherenkov radiator during the investigated discharges. The measurements were performed as a function of the detector position along the minor radius from r=60 mm (below the limiter located at r=85 mm) up to r=100 mm (near the chamber wall). Such measurements were not carried out for r<60 mm because the detector might be destroyed.

The experimental data, which were obtained for plasma of a relatively low-density, showed that in this case the fast electron flux rose up strongly for the detector radial positions at r < 80 mm. For plasma of a higher density (above 10^{19} m⁻³) the electron flux was lower, in particular for r = 60-80 mm.

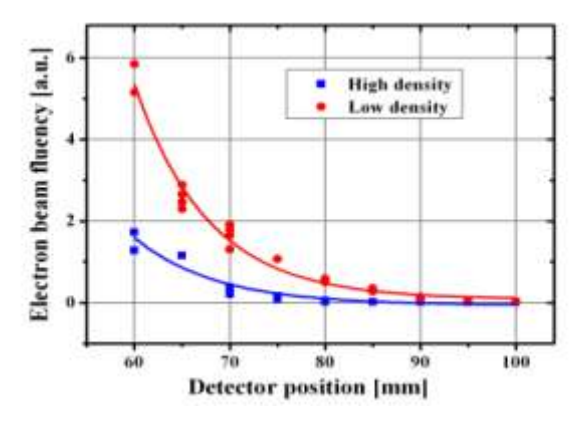


Figure 2 Dependence of the electron fluence on the position of the Cherenkov detector along the CASTOR minor radius, as recorded for the different values of the electron density $n_e \sim 6.5 \times 10^{18} \text{ m}^{-3}$ (red curve) and $1.2 \times 10^{19} \text{ m}^{-3}$ (blue curve)

A significant influence of the toroidal magnetic field value on particle confinement, and consequently on the plasma density in CASTOR-tokamak, was also observed and analyzed as reported at international conferences in Warsaw, Greifswald and Lisbon [1-3].

Ad c). In 2007 the CASTOR machine was shut down, and the TORE-SUPRA facility was not ready for Cherenkov measurements. Therefore, in order to get more experience in measurements of fast electrons in tokamak-type discharges, the use was made of an invitation to the IST in Lisboa, Portugal, in a frame of the EURATOM program. A Cherenkov-type measuring probe was prepared and installed within the ISTTOK facility. Preliminary measurements were carried out at different conditions during several experimental sessions in November and December 2007. Results of those measurements are now under the elaboration.

Conclusions

It can be concluded that the collected data are useful for the understanding of plasma behavior inside the CASTOR tokamak chamber. It can also be concluded that appropriate Cherenkov detectors might be applied for investigation of other tokamak-type facilities. One must, however, take into account experimental conditions and in particular thermal limitations during high-current discharges.

The first milestone, planned in the collaboration with the Association EURATOM/CEA (i.e. computational modelling of a heat transfer within the Cherenkov measuring head for TORE SUPRA experiments by means of a 3-D model), has been shifted until 2008 because of a lack of an software appropriate for future modelling. Two-dimensional numerical modelling of the heat transfer within a structure composed of diamond crystals and heat dissipator was carried out. The Cherenkov-radiators of complicated shapes were modeled by equivalent elements of the cylindrical symmetry. An influence of the heat transfer through contact surfaces was investigated.

The second milestone (i.e. design, manufacturing and tests of a prototype Cherenkov detector for the TORE-SUPRA facility, and preliminary measurements of fast ripple-born electrons) has been extended until 2008, according to the decision of our French partners. Measurements in the TORE-SUPRA were impossible because of a delay in the final assembling of the Cherenkov detector head and the manufacturing of the mobile shaft at CEA-Cadarache.

The third milestone (i.e. the elaboration of experimental results from measurements within the CASTOR and TORE-SUPRA facilities) was partially realized (in the CASTOR case). Results of this elaboration were presented in papers [1-3]. Instead of results from TORE-SUPRA (not available in 2007), there were elaborated some results of preliminary measurements performed within ISSTOC. Their detailed analysis is to presented in 2008.

Collaboration

Association EURATOM – IPP.CR, Prague, Czech Republic Association EURATOM – CEA, Cadarache, France Association EURATOM – IST, Lisbon, Portugal

- [1] L. Jakubowski, M. J. Sadowski, J. Stanisławski, K. Malinowski, J. Żebrowski, M. Jakubowski, V. Weinzettl, J. Stockel, M. Vacha, M. Peterka, Proc. EPS Conf. Warsaw, Poland, July 1-2, 2007, P5 097
- [2] J. Żebrowski, L. Jakubowski, M. J. Sadowski, K. Malinowski, M. Jakubowski, V. Weinzettl, J. Stockel, M. Vacha, M. Peterka, Proc. Intern. Conf. PLASMA-2007, Greifswald, Germany, Oct. 16-19, 2007, p. WeP3; AIP CP in print
- [3] L. Jakubowski, M. J. Sadowski, J. Stanisławski, K. Malinowski, J. Żebrowski, M. Jakubowski, V. Weinzettl, J. Stockel, M. Vacha, M. Peterka, Proc. 17th IAEA Technical Meeting on RUSFD, Lisbon, Portugal, Oct. 22-24, 2007, Book of Abstracts, p.63; AIP CP in print

2.7 Development and application of neutron diagnostics based on activation method for magnetic confinement devices

Marek Scholz Institute of Plasma Physics and Laser Microfusion, Warsaw marek@ifpilm.waw.pl

Adam Szydłowski, Sławomir Jednoróg, Rafał Prokopowicz, Lech Karpiński, Marian Paduch, Barbara Bieńkowska, Jacek Kaczmarczyk, Krzysztof Czaus, Witold Pawlak, and Ryszard Matulka

Abstract

The neutron activation technique is commonly used to determine neutron flux density and its spectrum. It is nowadays employed on JET mainly for calibration of time-resolved neutron yield detectors (fission chambers). In order to utilize this method more effectively and fruitfully some primary experiments were carried out on PF-1000 as well as on JET facility to test some other than traditionally exploited activation materials. It was shown that apart from indium, which is routinely exploited in this sort of measurements, such elements as Y, Er, Hf, Cd etc. can be successfully used in fusion experiments delivering more exact information about fluxes and also energy spectra of the analyzed neutrons. Especial effort was put to find activation materials with suitable cross sections $\sigma(E_n)$ and threshold energies (E_{th}) in the 0.5-3.0 MeV energy range to measure 2.5 MeV neutrons.

Summary

Neutron activation is the techniques for determination of neutron yields from magnetic confinement devices. One or more target foils are exposed to the radiation field for a predetermined period after which they are removed to a well-shielded counting station where the decay radiations can be recorded with the suitable detector for a period which depends on the decay half-lives. The advantage offers by the technique for the devices like JET or W7-X is that it is passive method, with the foil positioning and the decay radiation detection taking place during audit periods between discharge. The method is therefore free from mechanical, electrical, magnetic and radiation background problems. Unfortunately, the sensitivity of the method depends on number of emitted neutrons and a minimum expected neutron fluency at the irradiation point is $10^6 - 10^7$ n/cm². The foil activation method complements the measurements made with the time resolved neutron counters in two respects. First, the counters cannot be expected to follow all the fine details of the neutron production rate variations and thus will not provide an accurate measure of the total neutron yield in a discharge for which the production rate is highly erratic. Second, the multi-foil activation technique can be used to isolate neutrons of a particular energy, an essential feature lacking in the time resolved counters.

Measurement of neutron yield from deuterium plasmas at JET by activation techniques

The neutron activation technique has been used at JET for a long time mainly to determine local neutron fluence at certain measuring points. These measurements were supported by MCNP code in order to relate the neutron fluence to the total yield of neutrons from the plasma. The above method stayed to be more effectively after using by our self of many different elemental foils exposed simultaneously. There are exist a few nuclear reactions with threshold energy Ep in the range 0.5-3 MeV and relatively large cross-section values, e.g.: 89 Y(n,n') 89m Y, $E_p\sim1.0$ MeV, $T_{1/2}=15.7$ sec, 204 Pb(n,n') 204m Pb, $E_p\sim1.0$ MeV, $T_{1/2}=67.2$ min., 167 Er(n,n') 167m Er, $E_p\sim0.1$ MeV, $T_{1/2}=2.3$ sec. The report demonstrates promising results obtained with reactions as 180 Hf(n,n') 180m Hf, $E_p\sim0.1$ MeV, $T_{1/2}=5.5$ h, 111 Cd(n,n') 111m Cd, $E_p\sim0.3$ MeV, $T_{1/2}=48.5$ min., 27 Al(n,p) 27 Mg, $E_p\sim2.5$ MeV, $T_{1/2}=9.5$ min. Hafnium and yttrium have never been used in JET case and in other high temperature plasma experiments [1]. We have undertaken then an attempt to resume these investigations at JET.

Γ		lso-	Abun-		Daughter		
		tope	dance	Reaction	T _{1/2}		
	In	¹¹³ In	4.3%	¹¹³ In (n,n') ^{113m} In	99.5 m		
		¹¹⁵ In	95.7%	115 In (n,n') 115m In	4.5 h		
	Hf	¹⁷⁷ Hf	18.6%	¹⁷⁷ Hf (n,n') ^{177m} Hf	51.4 m		
				¹⁷⁷ Hf (n,n') ¹⁷⁷ⁿ Hf	1.1 s		
		¹⁷⁸ Hf	27.3%	¹⁷⁸ Hf (n,n') ^{178m} Hf	31 y		
				¹⁷⁸ Hf (n,n') ¹⁷⁸ⁿ Hf	4.0 s		
		¹⁷⁹ Hf	13.6%	¹⁷⁹ Hf (n,n') ^{179m} Hf	25.1 d		
				¹⁷⁹ Hf (n,n') ¹⁷⁹ⁿ Hf	18.7 s		
		¹⁸⁰ Hf	35.1%	¹⁸⁰ Hf (n,n') ^{180m} Hf	5.5 h		
	Er	¹⁶⁷ Er	23.0%	¹⁶⁷ Er (n,n') ^{167m} Er	2.3 s		
	Cd	¹¹¹ Cd	12.8%	¹¹¹ Cd (n,n') ^{111m} Cd	48.5 m		
	Y	⁸⁹ Y	100%	⁸⁹ Y (n,n') ^{89m} Y	15.7 s		
	Ni	⁵⁸ Ni	68.1%	⁵⁸ Ni (n,p)	9h →		
				^{58m} Co→ ⁵⁸ Co	71d		
	Au	¹⁹⁷ Au	100%	¹⁹⁷ Au (n,n) ^{197m} Au	7.7 s		
	Pb	²⁰⁴ Pb	1.4%	²⁰⁴ Pb (n,n') ^{204m} Pb	67.2 m		
		²⁰⁷ Pb	22.1%	²⁰⁷ Pb (n,n') ^{207m} Pb	0.8 s		
	Table 2. The calcuted meetingle and appropriate acceptions						

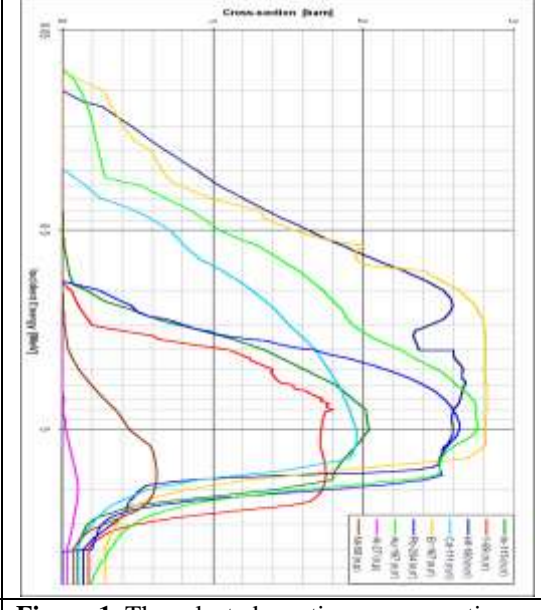


Table 3. The selected materials and expected reactions.

Figure 1. The selected reactions cross-sections.

Based up on MCNP code is obtained principal parameters of neutron fluence. It was also taken into account that the energy spectrum of neutrons, emitted from such source is described by a Gaussian-like distribution [4]. This modelling provided also, a so called, activation coefficients for some activators in particular irradiation ends [2], [3], [4], [5].

The capsule with the samples was removed from an irradiation end at the moment when the plasma current was switched off. It usually happened in a dozen or so seconds after the NBI heating pulse. The return of the capsule through the carousel took about 10 sec [6]. After that measurements of delay γ radiation were conducted. The measurements were made with pre-calibration HPGe detector system. Those allows to measure samples with different shape and density many times higher than 1 g·cm⁻³.

Neutron Activation Diagnostics for W7-X

So far only media with density close to 1g cm⁻³ were effectively measured and quantitative and qualitative analyze were performed until practical implementation of reported methodology. In IPPLM has been delivered method of activation and measurement of thick metal foils as the outstanding technique of neutrons fluency measurement. These method bases on activation of In, Cd, Au, Hf, Ag, Y, Br, Se, and measurement of an excited activation of the above nucleuses by the precalibrated HPGe system and some deconvolution of neutron spectra based on MCNP calculation [7], [8], [9]. This methodology allows to measure media with density range even dozens g cm⁻³ and any shape.

a. HPGe system and Laboratory Sourceless Calibration Software

System for neutron activation measurements allows measuring γ radiation from activated by neutron flux samples of plenty different materials. The above system consists on InSpector 2000 (I2K) multichannel analyzer (MCA), HPGe Coaxial Detector System, Genee-2000 Gamma Analysis Software (G2K), Pre-Calibrated HPGe detector, Labsocs Laboratory Efficiency Calibration Software.

The LabSOCS (Laboratory Sourceless Calibration Software) mathematical efficiency calibration software brings a new level of capabilities to HPGe sample assay in the laboratory by eliminating, or greatly reducing, the need for radioactive sources for efficiency calibration. By combining the detector characterization produced with the MCNP modeling code, mathematical geometry templates, and a few physical sample parameters, the LabSOCS Calibration Software gives researcher the ability to produce accurate quantitative gamma assays of most any sample type and size

b. Measurement technique

Measurements were made inside the shielding house made 100 mm of Pb with additional shielding made both from 1 mm Cd and Cu. The natural radiation background was measured in 24hours cycle. Detector background was measured just before sample inactivation in similar to the future researches

condition. This procedure allows to subtraction of sample and environmental radiation background from the activated sample radiation spectrogram. Energy and efficiency calibration of gamma spectrometer were completed with calibration source type MBSS-2 no.: 14032005-1000051 certificated by Czech Inspectorate for Ionizing Radiation. The efficiency calibrations of each particular activation detector were completed by gamma composer method. Each sample was placed on the central position horizontally on the top of detector in a special spot. These guarantee a full copy of measurement geometry from each particular measurement.

Based upon the above data is considered that a new category of neutron spectrometry method is delivered under international agreements.

Conclusions

In IPPLM has been implemented new technology of measurement neutron spectra based on activation technique and special analyze of delay γ radiation emission with sourceless calibration technology application. The accuracy of sourceless numerical method was successfully tested with Marinelli calibration source. The finally obtained millstones are as follows:

- The effective spectrometric system and powerful computing technique make the perfect compilation of our neutron activation laboratory.
- The size and shape of sample for activation must be in result of optimization process not as the authorities proposal like in case JET and FTU
- The highest material density the lowest effectiveness of gamma quantum registration by this same HPGe detector
- Delay gamma radiations from activation materials allow to perform quantitative and qualitative analyze and provide MCNP computation with wale data.

Collaboration

CSU EFDA – JET, Culham Science Centre, Abingdon, United Kingdom. Association EURATOM – ENEA, Energy Research Center, Frascati, Italy Association EURATOM – IPP, Greifswald, Germany

- [1] JET Interface Technical Review Documentation, Neutron Activation System (Diagnostic KN2), KN2/TCD/GS/19.1.83
- [2] Use of Activation Techniques for the Measurement of Neutron Yields from Deuterium Plasmas at JET, O. Jarvis et al., Fusion Technology, Vol. 20, Nov. 1991
- [3] Neutron Transport Calculations in Support of Neutron Diagnostics at JET, M. Loughlin et al., Review of Scientific Instruments, Vol. 70, No. 1, Jan. 1999
- [4] Calibration of Neutron Yield Activation Measurements at JET Using MCNP and FURNACE Neutron Transport Codes, M. Pillon et al., Fusion Engineering and Design 9 (1989) 347-352
- [5] Time-Integrated Yield Neutron Monitor for JET, O. Jarvis et al., AERE Internal Report G2094, 1982
- [6] Minutes of a progress meeting on the Activation System (KN2) for JET, 19thMar. 1985
- [7] R. Prokopowicz et al., "Measurements of neutron yield from deuterium plasmas at JET by activation technique", presented at Intern. Conf. PLASMA 2007, Greifswald, Germany, to be published by the American Institute of Physics.
- [8] M. Loughlin et al., "Neutron transport calculation in support of neutron diagnostics at JET", Review of Scientific Instruments, Vol. 70, No 1, January 1999.
- [9] J. F. Briesmeister, ed., MCNP A General Monte Carlo N-Particle Transport Code, Manual; LA-12625-M, Version 4B, Los Alamos National Laboratory 1997;

2.8 Applications of solid-state nuclear detectors (SSNDTs) for fast ion and fusion reaction product measurements in TEXTOR experiments

Adam Szydłowski
The Andrzej Sołtan Institute for Nuclear Studies
szydlowski@ipj.gov.pl

Aneta Malinowska, Katarzyna Małek, Karol Malinowski, Marek Rabiński, Marek J. Sadowski, and Mirosław Kuk

Abstract

The investigation of the behaviour of energetic charged particles (particularly 3 MeV fusion protons) in magnetically confined plasmas is very important for development of the magnetic fusion concept. Fusion reaction protons, which escape from the plasma, can be also used for the diagnostics of plasma parameters, and provide even more refined data than neutrons. Ion temperatures have been measured e.g. in PLT and TEXTOR devices from the broadening of the energy spectrum of 3-MeV protons generated in D-D nuclear reactions [1-2]. The most important is that fusion reaction products can be exploited to investigate populations of high-velocity fuel ions, which are accelerated by different heating processes. The energetic fuel ions, inducing nuclear reactions, induce distinct signatures on the fusion reaction neutron and proton energy spectra. These signatures can be observed in the energy spectra as low- and high-energy tails extending up to 7 MeV.

Summary

As far as the first experiment (Fig. 1A), revealed that the fusion-reaction protons are recorded upon the detector surface in a ring shaped area [3, 5], the second test (Fig. 1B) was performed in a series of shots especially deficient in the neutron (and fusion-proton) emissions. It was estimated that in the analyzed series (# 103397 - 103432) the neutron emission amounted merely to $Y_n \sim 10^{12}$ neutrons/day. So, the sample irradiated in the second test showed a very low track density, and it was not possible to determine precisely the track density distribution upon the sample surface. We were hardly able to estimate a histogram of track diameters, which were measured in many different spots upon the irradiated sample. In Fig. 1 there are presented the proton energy spectra, which were obtained from this histogram, taking into account the calibration diagram.

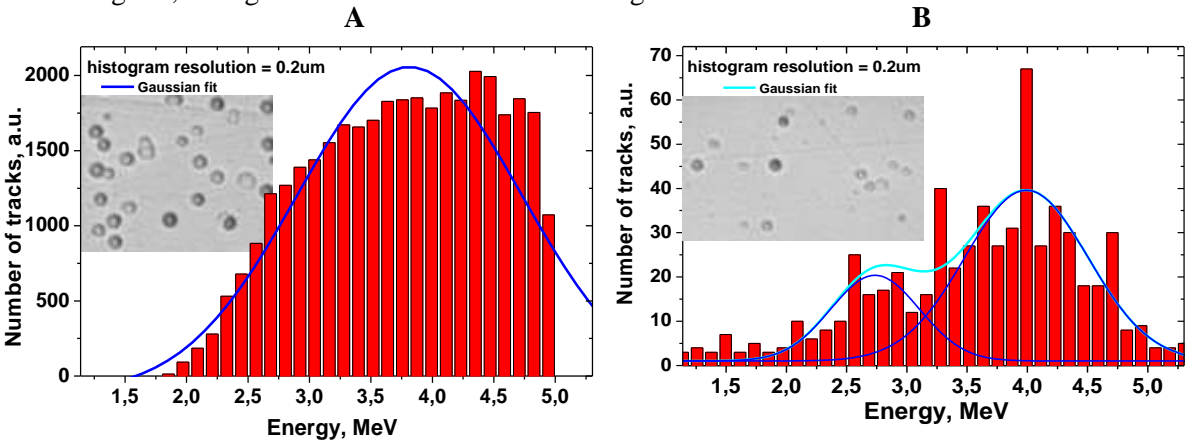


Figure 1 Energy spectra obtained on the basic of proton track diameters as measured upon detector samples, which were irradiated in the: A) first-; B) second- series within the TEXTOR facility.

The obtained spectra are considerably shifted towards higher energy regions, what can suggest that nuclear reactions were mainly produced by energetic reagents. In Fig. 3 there are presented the proton energy spectra, which was obtained from this histogram, taking into account the calibration diagram.

The undertaken measurements have been supported by the computations of the magnetic field configuration and proton trajectories within TEXTOR facility. The computer simulations have been performed on the basis of the particle motion equations using the Gourdon code. As a result the detector efficiency has been calculated as a function of the minor tokamak radius and particle initial pitch-angle (Fig. 2), for different spatial orientations of the camera entrance-pinhole. Presented numeric calculations were made in 2006 [4].

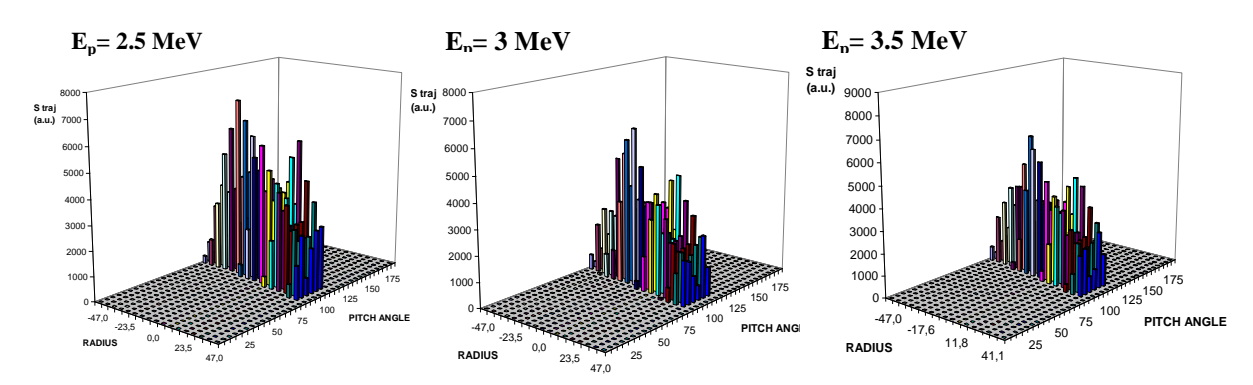


Figure 2 Distributions of the detection efficiency as were calculated for a detector in a ring shape ($r_{min} = 6.6$ mm, $r_{max} = 11.0$ mm) and for different proton energies (E_p), but the same orientation of the pinhole camera with respect to the major TEXTOR chamber radius ($\gamma = 0^0$)

Conclusions

The results of the described studies can be summarized as follows:

- 1. The solid-state nuclear track detectors of the PM-355 type appeared to be quite useful diagnostic tools also for Tokamak experiments, and the first measurements seem to be successful ones.
- 2. The detector samples irradiated with fusion-reaction protons in two different series of TEXTOR shots were subjected to the precise analysis with an optical microscope, and track density distributions and track diameter histograms were determined with a good accuracy.
- 3. Comparing the measured crater diameters with those induced by mono-energetic protons, it was possible to distinguish craters produced by protons from other craters and to convert the obtained histogram into the presented proton energy spectra.
- 4. The fusion proton spectra appeared to be shifted towards higher energy, what suggests that high energy reagents were responsible for nuclear fusion reactions occurring inside TEXTOR plasma.
- 5. Further measurement are needed (with different orientations of the pinhole camera) to get more information about nuclear reaction mechanisms and the spatial distribution of the fusion reaction rate.

Collaboration

Association EURATOM – Belgian State, ERM/KMS, Brussels, Belgium Association EURATOM – FZJ, Institute of Plasma Physics, Juelich, Germany

- [1] R. E. Chrien, R. Kaita, J. D. Strachan, Nucl. Fusion 23, 1399-1407 (1983)
- [2] G. Bonheure, ERM Laboratory Report No. 118, ERM, Brussels (2000)
- [3] A. Szydłowski, et al., Radiat. Meas., 2008 in press
- [4] G. Bonheure, A. Gałkowski, et al., Czech. J. Phys 56, B61-B65 (2006)
- [5] A. Szydłowski et al., IC PLASMA 2007, Greifswald, Germany Sept. 2007

2.9 C-O- Monitor for Wendelstein 7-X

Ireneusz Książek
Institute of Physics, Opole University
iksiaz@uni.opole.pl

Adam Bacławski, Tadeusz Kulig, and Józef Musielok

Abstract

A main fraction of impurity species in fusion plasmas originates from low-Z elements like carbon, oxygen, boron and nitrogen. The radiation of hydrogen-like ions of these elements can be an indicator for vacuum leakages as well as enhanced erosion of inboard tiles due to extreme local heat loads. It is therefore important to routinely monitor representative core-relevant spectral resonance lines (hydrogen-like ionization states) of these elements with high throughput and therefore high time resolution in order to avoid machine damage.

Therefore a fixed diagnostic is demanded, where no changes concerning wavelength or spatial position of viewing chords will be performed and which is exclusively reserved for fast monitoring of the lines of B V, C VI, N VII and O VIII. In order to perform tests of elements of the spectrometer under construction, the old "C-O- Monitor for Wendelstein 7-AS" have been revitalized and put into operation. After preliminary tests at IPP Greifswald the spectrometer have been transferred to Opole. Furthermore the work break schedule have been agreed.

Summary

The construction of "C- O- Monitor" requires suitable choice of its elements as the detector and dispersive element (crystal, grating or multilayer mirrors–MLM). Apart of detailed survey of existing solutions it is advisable to check new possibilities as recently constructed MLMs and detectors. In order to perform such tests the old "C- O- Monitor for W7-AS" have been revitalized and transferred to Opole.

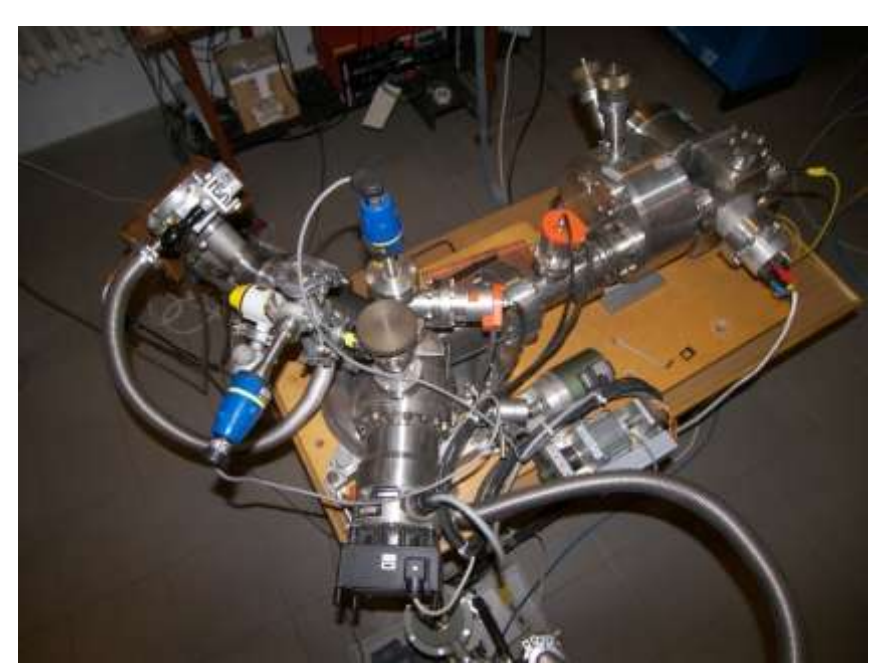


Figure 1 W7-AS X-Ray Monochromator with implemented X-Ray Tube

The "C- O- Monitor for W7-AS" is a crystal monochromator. The crystal is placed in a triangular chamber which is mounted onto the central ring of the goniometer. To the outer ring of the goniometer the detector housing is attached. The detector and vacuum housing are connected by flexible ballows. The crystal angle is fixed by turning the crank-handle, which results in setting the crystal at position α and the goniometer ensure simultaneously the detector to be set at angle 2α , so that Bragg's law is fulfilled.

The detector arm of the spectrometer carries a vacuum part that allows switching between two different detectors without breaking the vacuum. At the entrance of this "Y"-shape part a comb-like sollerslit reduces lower energy straylight or fluorescent radiation. This construction allows comparing signals obtained by two different detectors. Additionally, the special construction of one of the detector arms (containing shutter and set of valves) allows evacuating and venting this area without breaking vacuum of the whole spectrometer.

The spectrometer is currently connected to a low voltage (below 12 kV) X-ray tube of special construction,. The X-ray tube consists of a vacuum housing in which 3 selectable anode "fingers" can be inserted into the optical axis simply by turning the anode holder which is decoupled from the housing by a flexible ballow. Each finger contains a different anode material (Al, Fe and Cu) (2×3cm) and is bombarded by electrons from a iodized tungsten (tungsten+CsI) filament (cathode) which is mechanically supported and electrically supplied by the flange positioned opposite to that for the fingers. Each finger is cooled by pressed air (1.8 bar). The temperature of the cooling gas is controlled by thermocouples feedbacked with the high voltage power supply. The radiation emitted from the selected anode is collimated by the Soller-slit placed close to the crystal surface. In front of the collimator unit a filterbox has been installed which contains 21 different filters and apertures arranged in 3 successive layers. By selecting the filters one can attenuate the radiation emitted by the lamp and study the fluorescence radiation emitted from different foils (filters).

In order to operate the X-ray tube it is necessary to keep the vacuum in the spectrometer at 10⁻⁶ mbar. This vacuum is obtained by applying a set of pumps containing forepump and turbopump. The pressure in the spectrometer is controlled by two thermovac and two ionivac units.

Conclusions

After some check-up and necessary repair the "W7-AS X-Ray Monochromator with implemented X-Ray Tube" have been transferred to Opole. Its construction allows to apply this device in study and testing of:

- detectors,
- dispersive elements (e.g. measurement of crystal and MLMs rocking curve),
- soft X-ray radiation sources.

Collaboration

Association EURATOM - IPP, Greifswald, Germany

2.10 Microwave diagnostic development

Yury A. Kravtsov

Maritime University of Szczecin, Poland
kravtsov@am.szczecin.pl

Bohdan Bieg, Paweł Berczyński, and Janusz Chrzanowski

Abstract

Quasi-isotropic approximation (QIA) of geometrical optics method is presented, which describes evolution of electromagnetic waves in weakly anisotropic media. This method was generalized recently in different directions. At first, it is shown that in combination with paraxial complex geometrical optics QIA opens an unique opportunity to describe both polarization and diffraction changes of the electromagnetic waves in weakly anisotropic media. At second, QIA equations are presented in a compact form by involving the complex polarization angle (CPA). Relations between CPA and traditional angular parameters of polarization ellipse are established. Equations for CPA evolution are derived for inhomogeneous magnetized plasma accounting both Faraday effect and Cotton-Mouton phenomenon. At third, equations for Stokes vector evolution, which are widely used in plasma polarimetry, are derived directly from QIA, what demonstrates deep unity of two seemingly different approaches to the solution of polarimetric problems. In conclusion a few numerical examples are given, illustrating pure Faraday and pure Cotton-Mouton effects in homogeneous plasma, as well as the phenomenon of the normal modes conversion in the homogeneous plasma.

Summary

There exist two main approaches for description of electromagnetic wave propagation and polarization in weakly anisotropic media. The first of them is Budden's method, which deals with coupled wave equations for the components of the electromagnetic wave field. Coupled wave equations for weakly anisotropic media were suggested in [1] in the form of quasi-isotropic approximation (QIA) of the geometrical optics method. QIA was developed in depth in the review paper [2] and in the book [3].

Alternative approach – "Stokes vector formalism", have been developing by Segre for the purposes of plasma polarimetry, see, for instance, [4] -7]. Comparing two approaches mentioned [5], Segre has analyzed advantages and shortcomings of each technique, omitting yet their deep unity, if not equivalence. It was shown recently [6,7] that equation for Stokes vector evolution can be derived in a consequent way from the Maxwell equations on the basis of the QIA approach.

This Report sums up the theoretical achievements in the area of microwave plasma polarimetry, obtained by the Maritime University of Szczecin in 2006-2007. The Report includes first of all the brief outline of the QIA approach, which forms a basis for high frequency plasma polarimetry.

At second, the Report contains theoretical methods, suggested still in the Report-2006 [8], but improved, modified and published in 2007:

- combination of QIA with complex geometrical method, allowing simultaneously describing of polarization and diffraction processes [9];
- modernized form of the equations for the complex polarization angle and derivation of principally new equations for traditional angular parameters of the polarization ellipse [10].

At third, the Report includes three new elements of principal importance: (i) derivation of Stokes vector formalism (SVF) directly from QIA [6,7]; (ii) revealing of practical difference between QIA and SVF [11]; (iii) development of numerical methods for analysis of EM wave polarization in the inhomogeneous weakly anisotropic plasma.

Conclusions

Theoretical fundament for microwave plasma polarimetry is developed on the basis of quasi-isotropic approximation of geometrical optics, allowing for joint description of diffraction and polarization phenomena and for derivation of Stokes vector formalism from QIA. The results of the first numerical stimulations are presented, performed on the basis of QIA.

Collaboration

Association EURATOM – IPP, Greifswald, Germany

- [1] Yu. A. Kravtsov, "Quasi-isotropic geometrical optics approximation", Sov. Phys.— Doklady, 13(11), 1125-1127 (1969).
- [2] Yu. A. Kravtsov, O. N. Naida and A. A. Fuki, "Waves in weakly anisotropic inhomogeneous media: quasi-isotropic approximation of geometrical optics", Physics-Uspekhi, 39(2), 129-134 (1996).
- [3] A. A. Fuki, Yu. A. Kravtsov and O. N. Naida, Geometrical Optics of Weakly Anisotropic Media (Gordon & Breach, Lond., N. Y., 1997).
- [4] S E Segre and V. Zanza, "Derivation of the pure Faraday and Cotton–Mouton effects when polarimetric effects in a tokamak are large", Plasma Phys. Controlled Fusion 48 339–351 (2006).
- [5] S. E. Segre, "Comparison between two alternative approaches for the analysis of polarization evolution of EM waves in a nonuniform, fully anisotropic medium: magnetized plasma", Preprint RT/ERG/FUS/2001/13, 2001, ENEA, Frascati, Italy (2001).
- [6] K. Yu. Bliokh, D. Yu. Frolov, and Yu. A. Kravtsov, "Non-Abelian evolution of electromagnetic waves in a weakly anisotropic inhomogeneous medium", Phys. Rev. A 75, 053821 (2007).
- [7] Yu. A. Kravtsov, B. Bieg, K. Yu. Bliokh, Stokes-vector evolution in a weakly anisotropic inhomogeneous medium, J. Opt. Soc. Am. A 24(10) 3388-3396 (2007).
- [8] Yu. A. Kravtsov, B. Bieg, P. Berczyński, J. Chrzanowski. *Quasi-isotropic approximation of geometrical optics method with application to microwave plasma polarimetry*. In: Annual Report 2006, Association IPPLM-Euratom, p.39.
- [9] P. Berczyński, Yu. A. Kravtsov. *Microwave diagnostics of plasma: combination of quasi-isotropic approximation with complex geometric optics*. Dni Asocjacji Euratom-IFPLM, Kudowa Zdroj, 18-21 Sept. 2007.
- [10] Z. H. Czyż, B. Bieg and Yu. A. Kravtsov, "Complex polarization angle: relation to traditional polarization parameters and application to microwave plasma polarimetry", Phys. Lett. A 368 101-107 (2007).
- [11] Yu. A. Kravtsov, P. Berczyński, B. Bieg, K. Yu. Bliokh, Z. H. Czyż., *Polarization evolution in weakly anisotropic media: "quasi-isotropic approximation" (QIA) of geometrical optics method and its recent generalizations*. PIERS-2007, Prague, Charles Technical University, 27-30 Sept. 2007

2.11 Detection of the delayed neutrons from activation of fissionable materials in the neutron field at fusion-plasma devices

Krzysztof Drozdowicz The Henryk Niewodniczanski Institute of Nuclear Physics Polish Academy of Sciences krzysztof.drozdowicz@ifj.edu.pl

Barbara Gabańska, Andrzej Igielski, Władysław Janik, Ewa Krynicka, Arkadiusz Kurowski, Urszula Wiącek, and Urszula Woźnicka

Abstract

Neutrons emitted from fusion plasma bring information on parameters and behaviour of the plasma. The neutron activation method is in this respect a principal technique for fusion plasma diagnostics. This method can be supplemented with the detection of delayed neutrons from samples of fissionable materials irradiated in the same positions as samples for the activation analysis. A project is undertaken to design and built a device for detection of delayed neutrons from the irradiated samples. Physical and geometrical assumptions are defined and Monte Carlo simulations of the neutron transport and detection in the device are presented. This is a first step before the final optimization of the device which is to be installed at the Wendelstein 7-X stellarator.

Summary

The neutron activation method is a principal method for neutron-based techniques for fusion plasma diagnostics. The detection of the delayed neutrons from fissionable isotopes covers some gap in the neutron activation diagnostics which is made with the use of other elements and based on the gamma spectrometry of the activated samples. This delayed neutron method has been used at tokamaks, as *e.g.* at JET.

The new-generation stellarator, Wendelstein 7-X, being under construction in the Max-Planck-Institute for Plasma Physics, Greifswald Branch, will serve for research of the fusion plasma physics in connection to the international programme ITER. One of the aims of the W7-X project is to develop extensively methods of the plasma diagnostics.

A device for the delayed neutron detection will be built within the frame of the present project. It will be finally installed as a part of the neutron activation diagnostics system at the W7-X stellarator. Before the installation, the device will be tested and used for the plasma research at the Plasma-Focus source in the Institute of Plasma Physics and Laser Microfusion (Association EURATOM, Poland).

The idea of the measurement is following. A sample (tablet) of the fissionable material (as ²³⁵U, ²³⁸U or ²³²Th) is placed in an exposition location, close to the plasma or spread in the torus hall, and irradiated by neutrons coming from the D-D or D-T reactions. Then it emits prompt neutrons (~99 %) at the fission act and later the so-called delayed neutrons (~1%) from the fission products which decay with the beta-emission. Interpretation of the measured time distribution of the delayed neutron decay delivers information on the primary plasma-neutron field.

Preliminary assumptions for the device for detection of delayed neutrons have been formulated. An initial important part of the research before designing the device is performed by the computer simulation method. The numerical simulations are made using the Monte Carlo method for calculation of the transport of neutrons (and other particles) in the matter. The MCNP code is used for this purpose. Essential stages of the physical effects have been modelled, including geometry of the device, nuclear reactions in the activated tablets of fissionable materials, slowing-down and transport of neutrons through consecutive layers of the device to the neutron detectors, and detection of thermal neutrons. The shape of the measuring device has been assumed as a parallelepiped with the square cross-section. An inner chamber for the measured sample (which emits the delayed neutrons) is surrounded by a few layers of various materials which slow down the fast delayed neutrons and are a shield against outer radiation background (see Fig. 1).

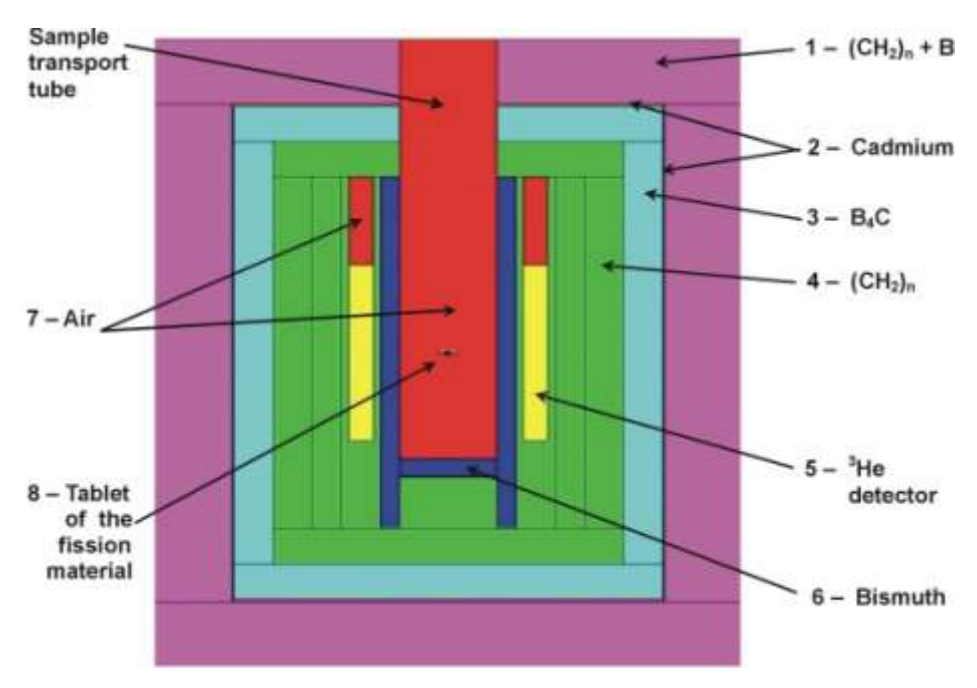


Figure 1 Schematic vertical cross section of the setup for the delayed neutron detection

The irradiation of the fissionable material tablets (cylindrical of three various shapes, containing U-235 or Th-232 in various amounts) was simulated using the MCNP code. Energy spectra of the arising delayed neutron were obtained. An example is shown in Fig. 2.

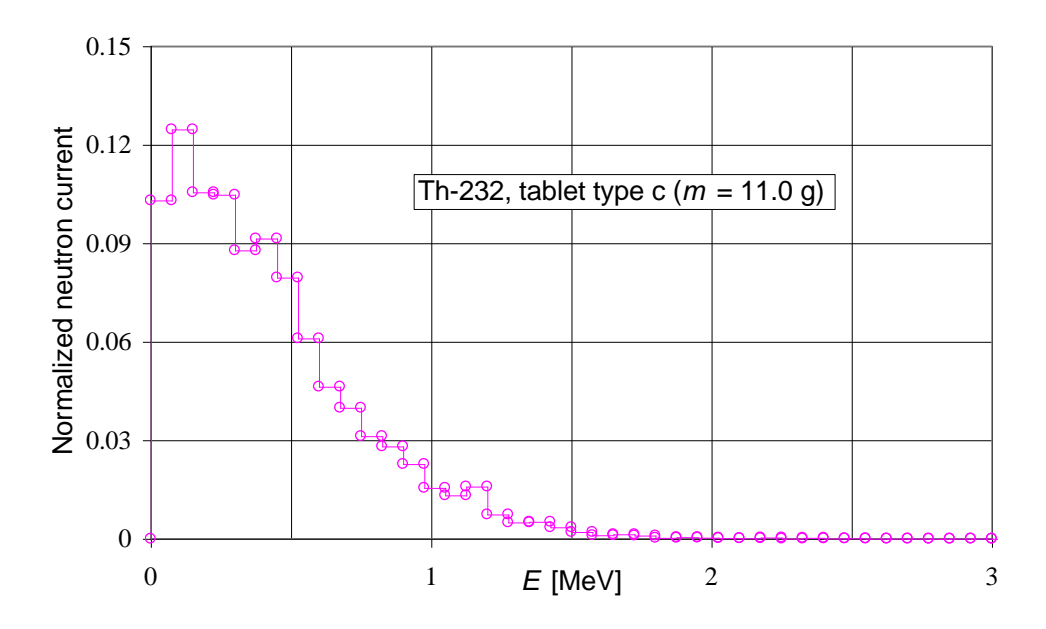


Figure 2 Energy distribution of the delayed neutrons from. Th-232 tablet type c

Conclusions

Input files with geometrical and physical data for the MCNP modelling were prepared:

- for simulation of the fission reactions with generating delayed neutrons in the tablets of fissionable isotopes,
- for simulation of neutron transport from the tablet to neutron detectors in the measuring device,
- for calculation of the detection efficiency,
- for determination of an influence of the external neutron radiation.

All these simulations were performed and the initial data for optimization of the device were in this way obtained. The number of necessary He-3 detectors was fixed. The amount of boron in polyethylene in the external protection layer was determined.

In the next step of the project, particular elements of the device have to be carefully optimized to get a maximum efficiency of the delayed neutron moderation and detection (width of the moderating layer, position of the neutron detectors inside the layer, etc.). Parts of the electronic setup are to be chosen in respect to the expected count rates and half-life times of the delayed neutrons.

For a final interpretation procedure, an influence of the use of various data of the nuclear crosssections on the absolute values and accuracy of the calculated efficiency of fission in tablets has to be investigated.

Collaboration

Association EURATOM – IPP, Greifswald, Germany EFDA JET, Culham, UK

2.12 Stellarator modelling

Roman Zagórski Institute of Plasma Physics and Laser Microfusion zagorski@ifpilm.waw.pl

Sebastian Głowacz, and Włodzimierz Stępniewski

Abstract

The FINDIF code is used to investigate the energy transport in the complex 3D geometries (W7-X, TEXTOR-DED). A numerical method based on the finite difference concept which uses an unstructured grid has been developed. The grid is generated by field-line tracing to guarantee complete decoupling between the parallel and perpendicular transport. A numerical meshes for W7-X stellarator and TEXTOR-DED tokamak have been prepared. Numerical simulations of energy transport have been performed for 12/4 and 6/2 modes of the TEXTOR-DED operation.

Summary

The work done in 2007 focused on the further development of the FINDIF code by implementation of the new explicit algorithm for solving the differential equations as well as on the extending the numerical model by adding to the already implemented electron and ion energy equations also continuity and momentum equations. It appeared however, that the new version of the code, still suffers from numerical problems. Therefore a large part of our effort in 2007 concentrated on improving the code and finding the reasons for numerical problems.

Since the new version of the code does not work properly, we have used an older version of FINDIF which solves only the temperature equations to investigate the energy transport in the boundary layer of TEXTOR-DED tokamak. The Dynamic Ergodic Divertor in TEXTOR [6] is an excellent tool to study the basic properties of the magnetically perturbed edge plasma region, which consists of magnetic field lines with dramatically different connection lengths. There is no clear boundary between the ergodic and laminar region, while the flux tubes formed by the long connection length field lines are adjacent to the flux bundles of laminar field lines. Numerical grids have been prepared in order to simulate experiment corresponding to the 12/4 and 6/2 modes of the DED operation, respectively.

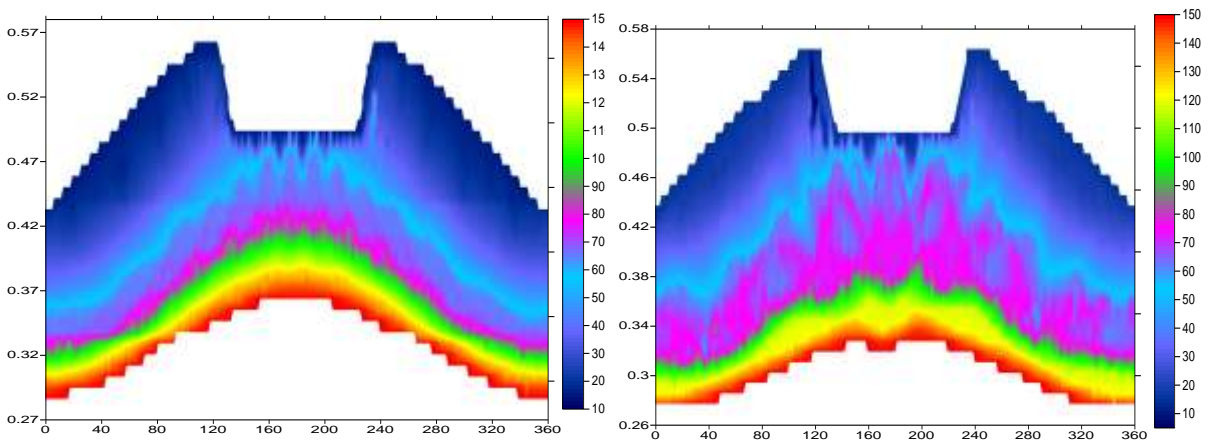


Figure 1 Distribution of T_e at the Poincare section (ϕ =0) **Figure 2** Distribution of T_e at the Poincare section (ϕ =0) for n_e =10¹⁸ m⁻³, mode 12/4 for n_e =10¹⁸ m⁻³, mode 6/2

Since in the present transport model the continuity and momentum equations are not fully implemented yet, we have solved the transport equations for Te and Ti for different values of the plasma density (n_e = 0.1, 1, 5 × 10¹⁹ m-3) in order to assess the effect of n_e on the energy transport. For the radial transport we have assumed constant conductivity coefficients being of the order of Bohm diffusion. It is apparent, that the magnetic topology is closest reflected in the solution of the electron

temperature field at $n_e=10^{18}$ m⁻³, (Figs. 1-2) which indicates that the parallel transport is dominant. If the density increases, in particular for Ti, the heat conductivity is reduced forcing the development of temperature gradients along field lines and in addition, the role of the radial transport increases leading to the stronger mixing of temperatures from different regions, and consequently the mesh details are less pronounced. However, the hot spot structure of the temperature distribution close to the target is always preserved.

Conclusions

The finite difference method has been applied to solve electron and ion energy transport in the complicated 3D TEXTOR-DED geometry. The implicit version of the FINDIF code using the free-point method to solve the radial transport has been applied to assess the properties of the heat transport in the edge of the TEXTOR-DED tokamak. It appears that the temperature distribution reflects the magnetic field line structure in the TEXTOR-DED boundary region reflecting the finger-like pattern of the laminar zone. In particular that effect is very visible for low plasma densities when the transport along the field lines is dominant and the temperature gradients are weak. With increasing plasma density, the parallel transport is reduced in respect to the radial one, and temperature gradients along the field lines start to develop leading to the mixing of the temperatures from different field lines and to the broadening of the ergodic region. It appears that in the case of TEXTOR DED the three-dimensional topology of the magnetic field lines, including the connection length and radial penetration of magnetic field lines, is very important. The radial penetration of the magnetic field lines within the Kolmogorov length is strongly correlated with the simulated distribution of the heat flux density over the target surface, which is well confirmed by experimental measurements [7].

Collaboration

Association EURATOM – IPP, Greifswald, Germany Association EURATOM – FZJ, Institute of Plasma Physics, Juelich, Germany

- [1] A. M. Runov et al., Phys. Plasmas, 8, (2001) 916.
- [2] R. Zagórski et al., Comp. Phys. Com., 164 (2004) 318
- [3] N. McTaggart, R. Zagórski, X. Bonnin, A. Runov, R. Schneider, T. Kaiser, T. Rognlien, and M. Umansky, "3D Edge Energy Transport in Stellarator Configurations", J. Nucl. Materials, vol. 337-339, (2005) p.221
- [4] K. Jach et al., "Computational modelling of the dynamical systems with the free-points method", Polskie Wydawnictwo Naukowe, Warsaw (2001) (in Polish)
- [5] R. Zagórski, M. Jakubowski, N. McTaggart, R. Schneider, W. Stępniewski, and P. Xanthopoulos, "Application of the 3D Finite Difference Scheme to the TEXTOR-DED Geometry", submitted to Contrib. to Plasma Phys.
- [6] Fusion Eng. Des. 37, 335 (1997). Special issue devoted to the DED, guest editor: K. H. Finken.
- [7] M. Jakubowski et al 2007 Plasma Phys. Control. Fusion 49 S109

2.13 Fast ion driven plasma modes – theoretical basis for integrated tokamak modelling

Irena Kruk
The Institute of Physics, Szczecin University of Technology
jarek@ps.pl

Paweł Berczyński, Hubert Fuks, Sławomir Marczyński, Rafał Z. Rogowski, and Jarosław Zaleśny

Abstract

In 2007 we focused on two-mode equations, succeeding in confirming modes competition and observed beat of modes.

Moreover, we simplified the integro-differential single mode equation to an ordinary differential equation.

Summary

The simplified single-mode equations were developed by Berk and Breizman more than ten years ago; since then, the equations have been the subject of considerable research [1,2]. However, the single-mode theory obviously does not describe the interactions between the modes. Collaborating with Prof. M. Lisak and Prof. P. Helander, our team concentrated on the development of Berk-Breizman's approach which would allow in future for the generalizing to multi-mode case. The system of the two nonlinear complex equations for plasma modes amplitudes A_1 , A_2 , derived in cooperation with Nonlinear Electrodynamics Group (M. Lisak and D. Anderson), had five independent parameters and has the following form:

$$\frac{dA_{1}(\tau)}{d\tau} = A_{1}(\tau)$$

$$-\int_{0}^{\frac{\tau}{2}} \tau^{2} \int_{0}^{\tau-2\tau_{a}} e^{-(2\tau_{a}+\tau_{b})\hat{v}} \left(A_{1}^{*}(\tau-2\tau_{a}-\tau_{b})A_{1}(\tau-\tau_{a})A_{1}(t-\tau_{a}-\tau_{b}) + A_{2}^{*}(\tau-2\tau_{a}-\tau_{b}) + A_{1}(\tau-\tau_{a})A_{2}(\tau-\tau_{a}-\tau_{b}) \right) d\tau_{b} d\tau_{a}$$

$$\frac{dA_{2}(\tau)}{d\tau} = A_{2}(\tau)$$

$$-\int_{0}^{\tau/2} \tau^{2} \int_{0}^{\tau-2\tau_{a}} e^{-(2\tau_{a}+\tau_{b})\hat{v}} \left(A_{2}^{*}(\tau-2\tau_{a}-\tau_{b})A_{2}(\tau-\tau_{a})A_{2}(\tau-\tau_{a}-\tau_{b}) + A_{1}^{*}(\tau-2\tau_{a}-\tau_{b}) + A_{2}(\tau-\tau_{a})A_{2}(\tau-\tau_{a}-\tau_{b}) \right) d\tau_{b} d\tau_{a}$$

$$(2)$$

$$+A_{1}^{*}(\tau-2\tau_{a}-\tau_{b})$$

$$\cdot \left(A_{2}(\tau-\tau_{a}-\tau_{b})A_{1}(\tau-\tau_{a}) + A_{2}(\tau-\tau_{a})A_{1}(\tau-\tau_{a}-\tau_{b}) \right) d\tau_{b} d\tau_{a}$$

Our research proved that these parameters can be reduced to a single one, and that the solutions possess specific properties; Moreover, we succeeded in proving the modes competition and observed beats. Numerical results were obtained by means of numerical codes: sm-2m-k-1, sm-2m-k-2, sm-2m-k-3, sm-2m-k-4, sm-2m-d-1, sm-2m-d-2, sm-2m-d-3, sm-2m-d-4, sm-2m-d-5. The calculations were performed on a cluster computer in the Stellarator Theory Group in Greifswald.

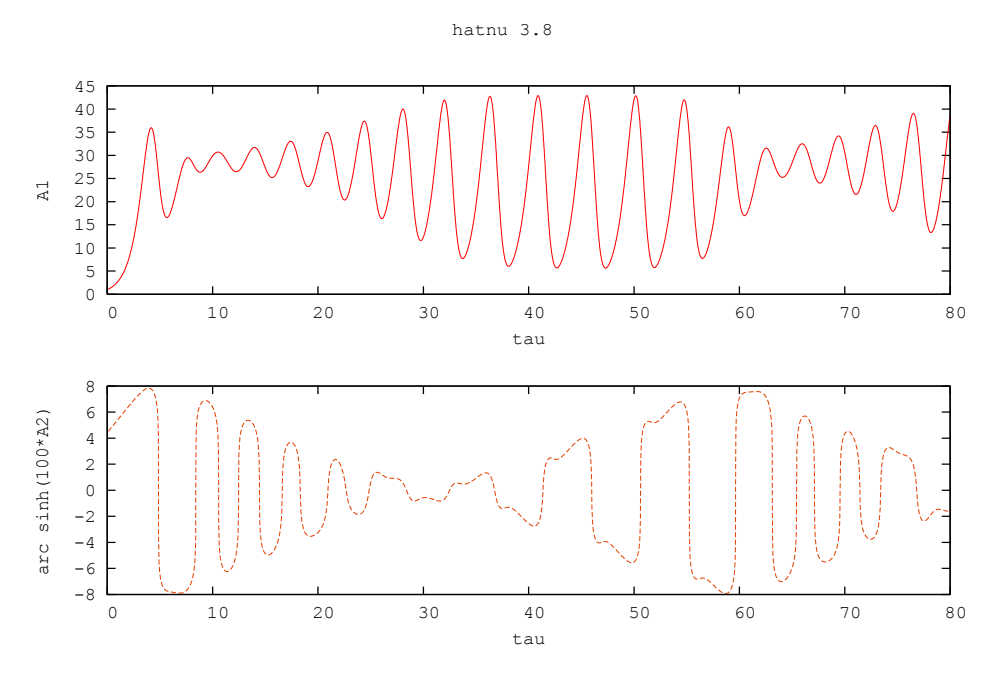


Figure 1 Numerical solutions of the system of equations (1,2) for the case of observed beats

The numerical calculations of original (BB) equation are very time consuming. Therefore, after some approximations, we have proposed some purely differential equation which contains all the essential physics of the (BB) theory. It radically shortened the time of numerical calculation from hours to seconds. Simplifying further the differential equation we reduced the (BB) instability problem to the instability of nonlinear oscillator. In this analogy the problem of damping of wave interacting with resonant particles was reduced to the sign of the damping coefficient of the nonlinear oscillator. In plasma physics language the negative sign of this parameter means that plasma wave gains energy from particles.

Conclusions

We analyzed the case of two waves interaction in the fusion plasma. We observed mode competition and beats in simulated numerical solutions. We simplified existing Berk-Breizman single-mode approach to the ordinary differential equations domain. Our results are going to be published in 2008 in a appropriate journal.

Collaboration

Association EURATOM – VR, Chalmers University of Technology, Göteborg, Sweden Association EURATOM – IPP, Greifswald, Germany

- [1] H. L. Berk et al., *Nonlinear Dynamics of a Driven Mode near Marginal Stability*, Phys. Rev. Lett. 8(76)1996, pp 1256-1259.
- [2] B. N. Breizman et al., *Critical nonlinear phenomena for kinetic instabilities near threshold*, Phys. Plasmas, 5(4)1997, pp (1559-1568).

2.14 Numerical analysis and evaluation of the structural mechanical behaviour of central support connections under electromagnetic forces for W7-X

Lukasz Ciupiński
Faculty of Materials Science and Engineering, Warsaw University of Technology
lukas@inmat.pw.edu.pl

Grzegorz Krzesiński, Piotr Marek, and Romuald Dobosz

Abstract

The objective of the Wendelstein 7-X (W7-X) project is construction of a stellarator which shall demonstrate that this type of reactor can be considered as future devices for energy supply. The design of the detailed coil-support connections has been a critical item for W7-X as even small deviations of the coils ideal shapes or non-symmetric alignments may cause magnetic field perturbations resulting in serious disturbance in operation of the device due to additional magnetic islands, uneven load of the divertor target plates or enhanced particle losses. Within the past years (2005-2006), structural analyses for all 14 CSEs have been performed by the Warsaw University of Technology. The sequence in which the 14 connections have been treated was governed by priorities set by the design status on the one, and by the severity of the structural loads and consequently the performance challenges to the connections on the other hand.

W7-X is currently under assembly in Greifswald. The major details of the design had been frozen in accordance with the ongoing component manufacture. Nevertheless, modifications to the design of CSEs are still needed and stem from assembly trials. Therefore, some of the CSEs have been reanalysed and new parametric models of 5 CSEs have been developed to enable fast, semi-automatic analysis for future design modifications and checks.

Summary

The following tasks have been performed in the year 2007:

- Final computations of the Double Connection Submodel (DCS) and Triple Connection Submodel (TCS) including part of coils
- Additional separate analyses of the coil welds for DCS and TCS
- Development and testing of semi-parametric models for analysis of 5 CSEs

The major efforts were concentrated on the development and testing of so called semi-parametric models of the 5 CSEs Those semi-parametric models enable an automated analysis of the connection and generate results in a standardized form, thus easy to compare. Each semi-parametric model of a connection consists of the ANSYS compatible database file and several macro files. It is also accompanied by a guiding document describing all macros and listing the parameters that can be altered for a given connection.

The following connections have been prepared as semi-parametric models:

- PA-Z1 and NPC1-Z1 as separate connections and double connection submodel
- PA-Z2 connection
- PB-Z2 connection
- PB-Z1 connection

As in every FE analysis the work with semi-parametric models starts with preparation of a geometric and discretesized models of the element to be analysed – a given CSE in this project. For geometry generation a specially prepared model of the connections – so called "basic model" using parametric description of the geometry, contact interfaces behaviour, material properties and loads have been developed.

The following parameters can be altered in the pre-processor phase:

- length of the sleeves and bolts (separately defined)
- all materials properties of the three materials (as functions of temperature)
- contact conditions for the three groups of interfaces (shim, wedges, other): gaps, contact stiffness, friction coefficients (temperature dependent)
- pretension forces in RT (individually defined)
- external forces applied (six components).

In the pre-processor phase the following four macros are used to prepare a connection model for calculations:

- 1. Scaling_and_Pretension.txt,
- 2. Change_Materials.txt,
- 3. Change_Contacts.txt,
- 4. Loads_and_Steps.txt

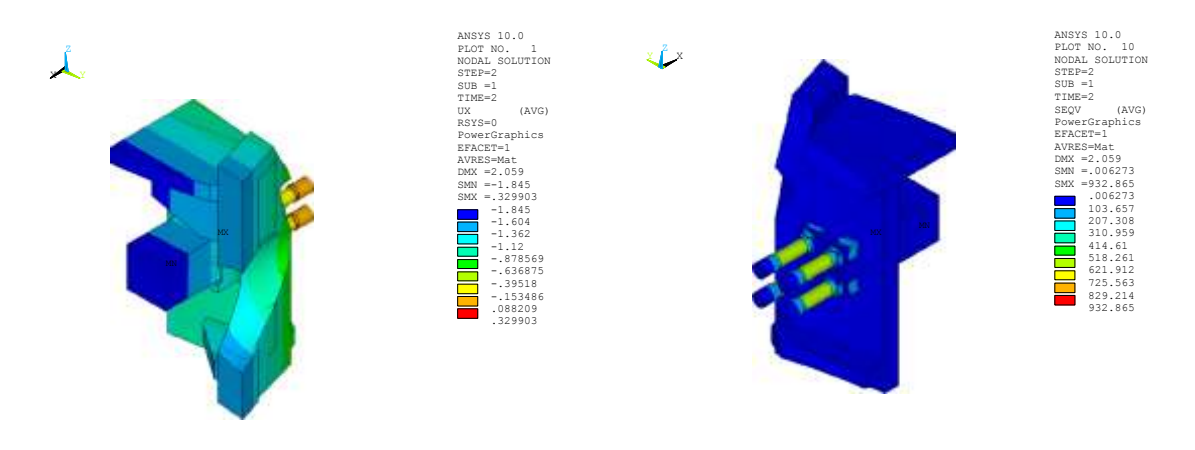
After executing the macros of the above list the model is ready for calculations which should be launched manually. Finally, in order to get results in standardized form the following series of macros should be executed in post-processor phase:

- 1. Bolts Stress Forces.txt,
- 2. Wedges_Stress_Forces.txt,
- 3. Shim_Displ_Stress_Forces.txt,
- 4. Path_Wedge_Weld_Stress.txt,
- 5. Path_Weld_Stress.txt,
- 6. Global_Results.txt.
- 7. Plastic Strain.txt,
- 8. Wedges_Contacts.txt,

The post-processor macros provide results in standardized form for all important elements of the connections as exemplified in table and figure below.

Table in the file Table_Bolt_Forces.txt

BOLT	FORCES C	F THE PB	-Z1 CONNECTION	
No.	FX	FY F	Z	
2.	251359.8 251353.7 251362.0 251353.6	-19.2 19.1	16.9 -17.6	



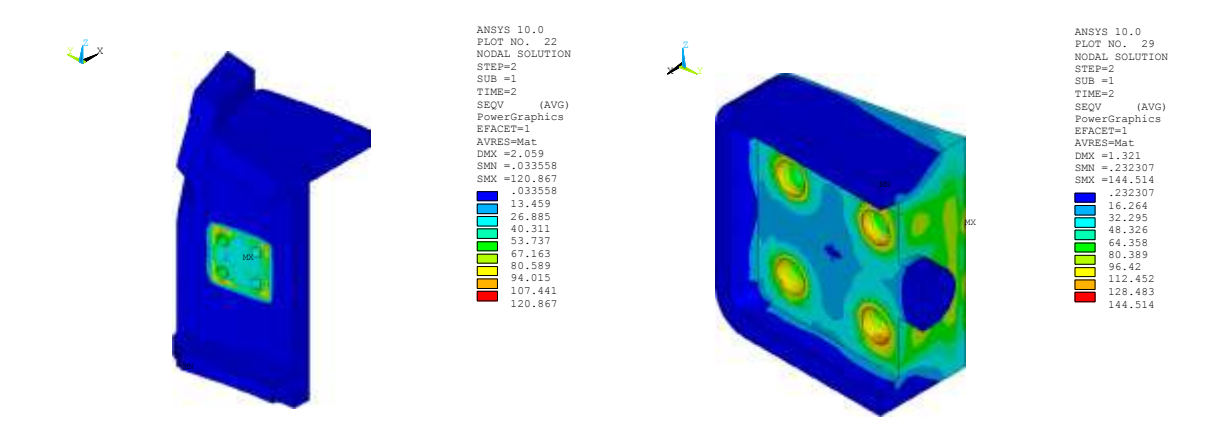


Figure 1 Some plots from the file Global Results.grph. Displacements and stresses within connections and its parts

The semi-parametric models for the connections have been tested. The tests consisted of re-running calculations of a given connection with the same set of input parameters for semi-parametric model as used in past for the "standard" model of the connection analysed in the past. The results of both, the semi parametric and "standard", models were then compared. All 5 semi-parametric models performed well in the tests.

Conclusions

A usefull tool – the semi-parametric model – for analysis of design changes in the 5 CSEs have been developed. The tool enables quasi-automatic analysis of the connection and generates results in a standardized form. This tool have already been used by System Integration team at Greifswald for the assessment of the latest design changes resulting from the assembly trials.

Collaboration

Association EURATOM - IPP, Greifswald, Germany

2.15 Investigation of the properties of high-Z Hohlraum-like plasma with the use of ion and X-ray diagnostics

Jerzy Wołowski Institute of Plasma Physics and Laser Microfusion wolowski@ifpilm.waw.pl

J. Badziak, L. Dereshwar, I. Foeldes, A. Kasperczuk, E. Krausky, L. Laska, K. Masek, P. Parys, M. Pfeifer, P. Pisarczyk, T. Pisarczyk, M. Rosiński, L. Ryć, R. Suchańska, L. Torrisi, and J. Ullschmied

Abstract

Production of heavy ion fluxes at the interaction of 70 J, 0.438 μm subnanosecond laser pulse with a massive planar target has been investigated using the time-of-flight method and three-frame interferometry. It is found that after proper optimization of high-Z (Cu or Ta) target irradiation, a highly collimated, energetic (0.1 – 1 MeV) heavy ion beam of the ion current > 100A and the ion current density > 1A/cm² at 1m from the target can be produced with an energy conversion efficiency nearly 10%.

Summary

Generation and study of ion beams from high-intensity laser-plasma interaction is rapidly developing into a frontier area stimulated by a variety of potential applications including ICF. Up to now, the highest currents (i_i) and current densities (j_i) of heavy ions in the far expansion zone $(\sim 1\text{m})$ were produced with the use of long (subns and ns) laser pulses interacting with massive targets [1, 2]. In this work, we show that at specific conditions of irradiation of high-Z target by a short-wavelength laser pulse, a highly collimated heavy ion beam of $j_i > 1\text{A/cm}^2$ and $i_i > 100\text{A}$ at 1m from the target can be generated with a high energy conversion efficiency $(\sim 10\%)$ at intensity $\sim 10^{14}\text{W/cm}^2$ and energy $(\sim 70\text{J})$. This effect must be considered in optimisation of indirect inertial fusion.

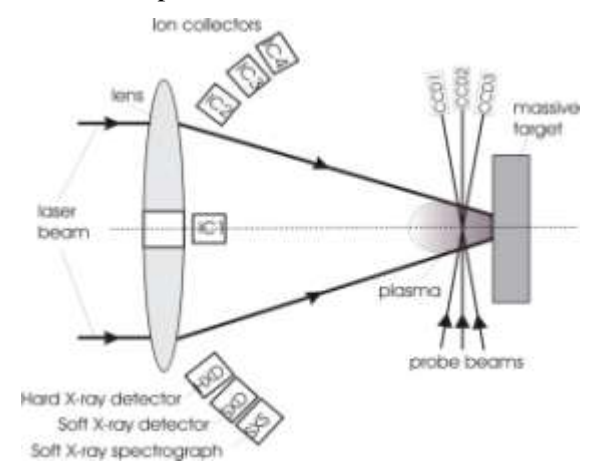


Figure 1 Simplified scheme of the experimental setup (out of scale)

This report presents results of the experiment on heavy ion beam generation with 3ω beam of the PALS iodine laser in Prague. Characteristics of plasma produced by the interaction of 70-J, 0.3-ns laser pulse with solid targets (Cu, Ta, Al or CH) were measured with the use of the time-of-flight method, three-frame interferometry and X-ray diagnostics (Fig.1). It is shown the after a careful optimisation of the conditions of irradiation of a high-Z target by a subns laser pulse, a highly collimated ($\Theta_i \leq 10^\circ$) energetic (0.1 – 1 MeV) heavy ion beam of $i_i > 100A$ and $j_i > 1A/cm^2$ at 1 m from the target can be generated with a high efficiency approaching $\sim 10\%$.

As it results from our previous measurements, performed at similar laser intensities with the use of the electrostatic ion-energy analyzer [3], the recorded ion flux is dominated by Cu ions of the maximum charge state $z_{max} \sim 20-25$. The IC signals also contain contaminant ions (mostly protons). The minimum, maximum and mean energies of Cu ions equal approximately 13keV, 1.3 MeV and 100keV respectively. The generation of highly collimated ion jets was observed only under specific conditions of the laser-target interaction, and particularly when: (a) the laser beam diameter on the target, d_L, was sufficiently large, (b) high-Z (Cu or Ta) target was used (we did not observe distinct ion jets from Al and plastic targets for the laser beam diameters applied in the experiment, i.e. of $d_L \le 800 \mu m$), (c) the laser focus was behind the target surface (for laser intensities on the target $\sim 10^{14} \text{W/cm}^2$ or higher). For the case of the large-aperture beam, the thickness of the overdense pre-plasma is remarkably small so the critical plasma surface is relatively flat. However, when the laser spot decreases, the critical surface curvature increases. The laser beam interaction with such a strongly curved critical surface prevents generation of highly collimated plasma (ion) beam. An explanation of the influence of the target atomic number on the ion (plasma) beam collimation is more complex. One of plausible mechanisms favourable to the beam collimation is a radiative cooling of plasma during the beam formation [4] which is more intense for the high-z plasma.

The influence of the laser focus position FP on the ion beam collimation can be explained taking into account the essentially different conditions for the interaction of the laser beam with the underdense preplasma (produced by the laser pulse leading edge) at FP(+) and FP(-). When the focal plane is placed in front of the target surface (the case FP(-)), the laser beam hits the preplasma at the peak laser intensity $> 10^{15} \text{W/cm}^2$. This intensity and the laser power ($\sim 3 \times 10^{11} \text{W}$) are both well above the thresholds for laser beam ponderomotive self-focusing in plasma [5]. Due to self-focusing, the laser beam intensity in the vicinity of the beam axis considerably increases. This results in the significant increase in radial components of both ponderomotive and termokinetic forces in the plasma, which prevents the expanding plasma (ion) flux collimation along the axis. In the case of FP(+) the laser beam intensity in the preplasma is several tens times smaller than in the case of FP(-) and self-focusing is insignificant. Thus, the conditions for quasi-planar acceleration of plasma in the case FP(+) should be much better than at FP(-).

Conclusions

It has been shown that after proper optimization of the conditions of irradiation of a high-Z target by a short-wavelength, 70 J, subns laser pulse, a highly collimated ($\Theta_i \leq 10^\circ$) energetic (0.1 – 1 MeV) heavy ion jet of $j_i > 1$ A/cm² and $i_p > 100$ A at 1 m from the target can be generated with a high energy conversion efficiency approaching ~ 10%. Radiative cooling of the expanding high-z plasma acts in favour of the ion jet collimation, while laser beam self-focusing in the plasma seems to be the main effect, which hinders it. To our knowledge the measured heavy ion currents and current densities are the highest among the ones achieved up to now in laser-plasma experiments. The production of highly collimated multi-MeV heavy ion jets of even higher ion currents and current densities seems to be feasible using short-wavelength subns laser pulses of energies in the 0.1 – 1 kJ range.

Collaboration:

Association EURATOM – IPP.CR, Prague, Czech Republic University of Messina, Messina, Italy PALS Research Centre ASCR, Prague, Czech Republic

- [1] L. Laska, et al., Rev. Sci. Instrum. 75, 1546 (2004)
- [2] J. Badziak, Opto-Electron. Rev. 15, 1 (2007)
- [3] J. Wołowski, et al., Plasma Phys. Control. Fusion 48, B475 (2006)
- [4] Ph. Nicolai, et al., Phys. Plasmas 13, 062701 (2005)
- [5] H. Haseroth, and H. Hora, Laser Part. Beams 14, 393 (1996)

2.16 Studies on fast ignition of inertial fusion using laser-driven proton beams

Jan Badziak Institute of Plasma Physics and Laser Microfusion badziak@ifpi lm.waw.pl

S. Jabłoński, P. Parys, M. Rosiński, J. Wołowski, P. Antici, J. Fuchs, and A. Mancic

Abstract

Generation of high-current proton beams of parameters scalable to those required for fast ignition of a fusion target was studied numerically and experimentally. Using a hydrodynamic relativistic 2D code, it was found that laser-induced skin-layer ponderomotive acceleration (SLPA) makes possible to produce collimated proton beams of MA currents and TA/cm^2 current densities at relativistic laser intensities above 10^{19}W/cm^2 . The production of proton beams of such extreme parameters was demonstrated in the experiment performed on the LULI 100TW laser facility, in which a subpicosecond laser pulse of intensity of $2\times10^{19} \text{W/cm}^2$ was used as the proton beam driver. Based on these results, a concept of ICF fast ignition using SLPA-produced proton beams was proposed.

Summary

Laser-driven proton fast ignition of fusion targets requires collimated proton beams of moderate proton energy ($\leq 10 \text{MeV}$) but of enormous proton current ($\geq 100 \text{MA}$) and current density ($\geq 10 \text{TA/cm}^2$) [1]. Generation of proton beams of such extreme parameters seems to be possible using the method referred to as skin-layer ponderomotive acceleration (SLPA) [2, 3].

Using a two-dimensional relativistic hydrodynamic code, production and focusing of proton beams driven by the SLPA mechanism at relativistic laser intensities was analyzed. It was shown that the key parameter determining the spatial structure and angular divergence of the proton beam is the ratio d_L/L_n , where d_L is the laser beam diameter and L_n is the plasma density gradient scale length. When $d_L \!\!>\!\! L_n$, a dense highly collimated megaampere (MA) proton beam of the proton current density approaching TA/cm² can be generated by SLPA at laser intensities above $10^{19} W/cm²$. The SLPA-driven high-current proton beams can be effectively focused by curving the target front surface. The focused beam parameters essentially depend on the density gradient scale length of the preplasma L_n and the surface curvature radius R_T . When $L_n \leq 0.5 \lambda_L$ (λ_L is the laser wavelength) and R_T is comparable with the laser beam aperture d_L , a significant fraction of the accelerated protons is focused on a spot much smaller than d_L , which results in a considerable increase in the proton fluence and current density [4].

In the experiment, performed on the LULI 100TW laser facility, a 350-fs, 1.05- μ m laser pulse of energy up to 15 J and intensity up to 2×10^{19} W/cm² irradiated a thin (1–3 μ m) PS (polystyrene) or Au/PS (PS covered by 0.05–0.2 μ m Au front layer) target along the target normal. It was found that the proton beams of MA currents and TA/cm² current densities at the source can be produced when the laser-target interaction conditions approach the SLPA requirements [5] (Fig. 1). The current and energy spectrum of protons remarkably depend on the target structure. In particular, using a double-layer Au/PS target results in two-fold higher proton currents and higher proton energies than in the case of a plastic target.

Based on the above results, a concept of ICF fast ignition using SLPA-driven proton beams was proposed [6]. According to this concept, the DT fuel compressed to the density of $300-400 {\rm g/cm^3}$ by cone-guided implosion is ignited by an ultraintense, focused proton beam generated at the interaction of a multi-PW/ps laser beam with a dielectric hydrogen-rich target of the curved front surface. To achieve the ignitor (proton beam) and fuel parameters required for the ignition, an implosion laser of energy $\sim 200 \ {\rm kJ}$ and an ignition (PW/ps) laser of energy $\sim 100 \ {\rm kJ}$ is necessary [6].

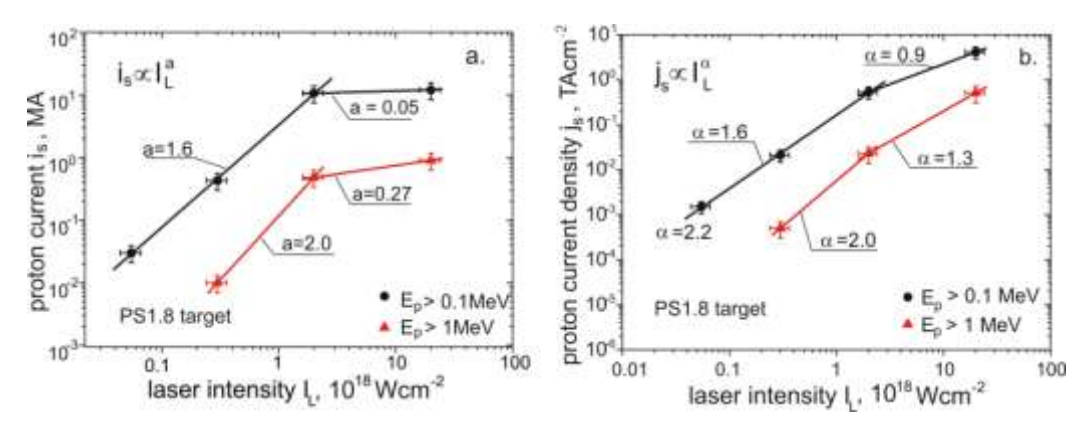


Figure 1 The proton beam current (a) and current density (b) at the source as a function of laser intensity. Points – the results of IC measurements; lines – the results of approximation by a power function

Conclusions

- SLPA makes it possible to produce highly collimated (or focused) dense proton beams of extremely high currents and current densities which are significantly higher than those produced by other methods currently known. In particular, the proton beams of MA currents and TA/cm² current densities at the source can be produced at laser energy only ~ 10J and laser intensity ~ 10¹⁹ W/cm².
- Parameters of SLPA-driven proton beams (current, intensity, mean energy etc.) as well as the laser-protons energy conversion efficiency can be significantly improved by using structured (eg. double-layer) targets.
- The production of SLPA-driven MeV proton beams of proton currents and current densities approaching those required for fast ignition of ICF targets (i.e. $i_p > 100 \, \text{MA}$, $j_p > 10 \, \text{TA/cm2}$), seems to be feasible at the near future when high-contrast multi-PW laser pulses will be available.

Collaborations

Association EURATOM – CEA, LULI, Palaiseau, France Association EURATOM – CIEMAT, UPT, Madrid, Spain Association EURATOM – IST, Lisbon, Portugal

- [1] M. Temporal et al., Phys. Plasmas 9, 3098 (2002)
- [2] J. Badziak et al., Plasma Phys. Control. Fusion 46, B541 (2004)
- [3] J. Badziak et al., Appl. Phys. Lett. 89, 061504 (2006)
- [4] J. Badziak and S. Jabłoński, Appl. Phys. Lett. 90, 151503 (2007)
- [5] J. Badziak et al., paper ThPo79, 5th IFSA Conference, September 9 14, 2007, Kobe, Japan
- [6] J. Badziak et al., Plasma Phys Control. Fusion 49, B651 (2007)

2.17 Formation of plasma jets and their interaction with ambient media

Tadeusz Pisarczyk
Institute of Plasma Physics and Laser Microfusion
pisaro@ifpilm.waw.pl

Andrzej Kasperczuk, Stefan Borodziuk, Daniel Baran, Hanna Włodarczyk, Joanna Pokorska, and Jan Pietrzak

Abstract

Experimental investigations of plasma jet parameters and plasma jet–ambient media interactions were carried out at the PALS laser facility. The optimization of the plasma jet parameters by changing target irradiation conditions constituted the first stage of our experiments. The experiments were performed with using the third harmonic of laser radiation (0.438 μ m) with pulse duration of 250 ps (FWHM). In order to optimize the plasma jet parameters, the laser beam energy and the focal spot radius were changed in the ranges of 13-160 J and of 35-600 μ m, respectively. Besides, the focal point was located both before and inside of the targets. The study was performed with the use of target materials of different mass densities (Cu, Ag, and Ta). Next, the optimized Cu plasma jets were used for a shock wave generation in ambient gases of different pressures. A high pressure supersonic gas nozzle was used to create a cylindrical column of argon or helium at densities varying from 10^{17} to 10^{19} cm⁻³.

Information about geometry of plasma expansion, plasma dynamics and electron density distributions were obtained by means of a 3-frame laser interferometric system. To have information about an actual laser intensity distribution on the target surface, a Photonic Science PE7051 x-ray pinhole camera and the crater replica method for reconstruction of a crater shape were used.

Our experiments have shown that the plasma jet forming is a fundamental process which accompanies the expansion of the laser plasma produced by irradiating a massive planar target, made of material of a relatively high atomic number, with a partly defocused laser beam. One can suppose that there are no laser energy limitations for the plasma jet creation because for all laser energies from the range used in the experiment the very well formed plasma jet was produced.

Interactions of the plasma jet with the ambient gases were performed for normal and ambient incidences of the laser beam in respect to the target surface. The exemplary results of the jet action on He and Ar gases in the case of the normal incidence of the laser beam are presented. They demonstrate processes creation and propagation of the shock wave in the gases at the front of the plasma jet. The experiments performed at the PALS laser system have shown that the supersonic plasma jets produced very simply in laboratory conditions, using the method proposed by authors of projects, can constitute a convenient tool in both the astrophysical and the inertial confinement fusion investigations.

Summary

The investigation of supersonic plasma jets production in laboratory conditions becomes a fundamental issue in both the astrophysical and the inertial confinement fusion contexts. Recently, we have reported on a simple method of jet production by interaction of a relatively low-energy laser pulse with a massive planar metallic target. This paper is devoted to optimization of plasma jet parameters and plasma jet–ambient media interaction which were carried out at the PALS laser facility. The experiments were performed at the third harmonic of laser radiation (0.438 μ m) with pulse duration of 250 ps (FWHM).

The optimization of the plasma jet parameters by changing target irradiation conditions was the first stage of our investigations. In order to optimize the plasma jet parameters, the laser beam energy and the focal spot radius were changed in the ranges of 13-160 J and of 35-600 µm, respectively. Besides, the focal point was located both before and inside of the targets. To test the influence of the focal point position on the plasma properties, two distances of the focal point from the target surface were chosen:

 $\pm 960~\mu m$ and $\pm 1630~\mu m$. They correspond to the beam spot radii on the target surface of 250 μm and 400 μm , respectively. The study was performed with the use of target materials of different mass densities (Cu, Ag, and Ta).

Our investigations allow us to come to the following conclusions:

- When the focal point is located inside the target, for all the materials used the jet forming starts at the focal spot radius (R_L) close to 200 μm . On the basis of our investigations concerning all the target materials used one can ascertain that the longest plasma jets with the smallest diameters and relatively high electron density are formed at R_L =300 μm .
- The capability of the plasma jet forming does not depend on the laser energy. For all the energies used in the experiment the parameters of the plasma jets produced under the same target irradiation conditions have well reproducible parameters.
- At the beam spot radius of 250 µm the plasma plume shapes for the positive and negative focal point positions differ considerably. If the focal point is located inside the target ("plus" position) the plasma stream consists of a wide part in the target vicinity (a jet pedestal) and of a narrow structure (a plasma jet) elongated considerably along the axis. If the focal point is set to the "minus" position the jet-like part of the plasma stream is practically absent. The situation changes substantially if the beam spot radius of 400 µm is applied. For the "plus" position of the focal point a characteristic long plasma jet is created, however of much larger diameter and, therefore, of much lower electron density. Evidently, the conditions are not proper for the jet forming in the latter case. On the other hand, at the "minus" focal point position nice jets are formed, similar to those observed for the "plus" position at R_L(+)=250 µm.

The investigations of the interaction of the plasma jet with ambient gases were carried out at the optimum conditions for the jet forming, i.e. the laser energy of 100 J, the focal spot radius of 300 μ m and the focal point situated inside the target. A high pressure supersonic gas nozzle was used to create a cylindrical column of argon or helium at densities varying from 10^{17} to 10^{19} cm⁻³. The gaseous targets with diameter of about 3 mm were produced in front of the Cu massive planar target at the distance of 3.5 mm. In Fig. 1 the exemplary results of the jet action on both gases in the case of the normal to the target surface incidence of the laser beam are presented.

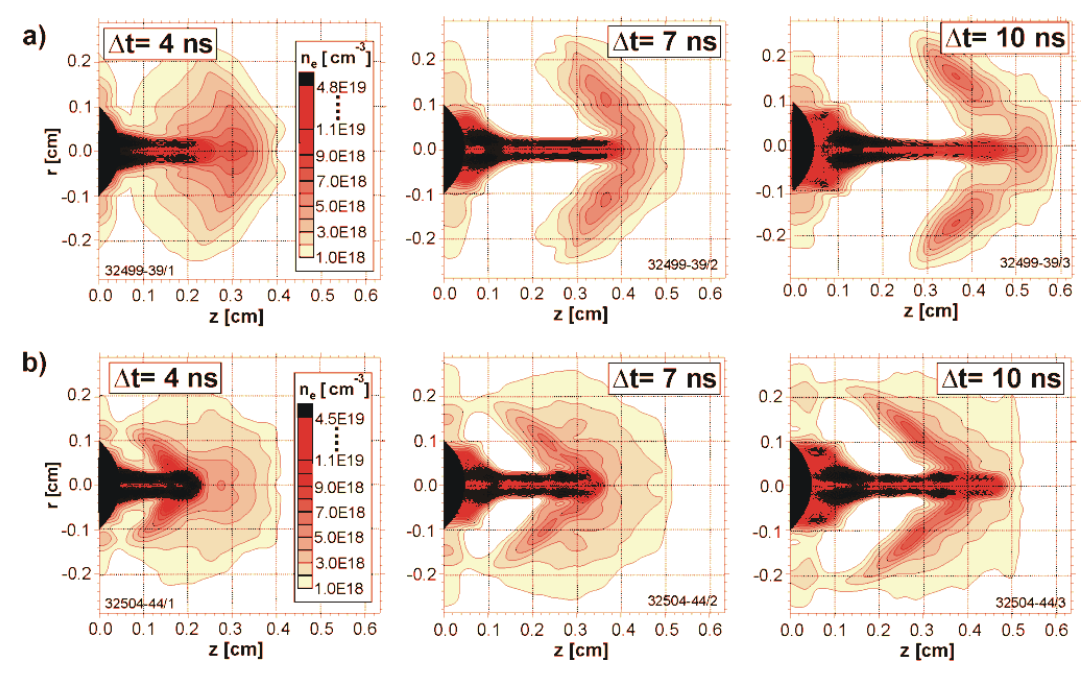


Figure 1 Selected results of the Cu plasma jet – gaseous targets interaction for He at pressure of 10 bar (a) and for Ar at pressure of 2 bar (b)

The electron equidensitograms demonstrate processes creation and propagation of the shock wave in the gases at the front of the plasma jet. The shock waves have usually a conical shape and thickness of 1-1.5 mm. The flat plasma front ahead the shock wave corresponds to the plasma originating from the direct laser beam action on the gases. The above results confirm that proposed by us the very simple method of plasma jet forming opens possibilities of universal applications of jets in physical investigations. Particularly, it concerns the astrophysical investigations where the plasma jets created in laboratory conditions can be scalled to real astrophysical conditions so as to know better nature of cosmic plasma jets and their interaction with other astrophysical objects.

Conclusions

Our experiment has shown that the plasma jet forming is a fundamental process which accompanies the expansion of the laser plasma produced by irradiating a massive planar target, made of material of a relatively high atomic number, with a partly defocused laser beam. At producing the plasma jets the focal spot radius can be changed over a wide range, but its optimum value seems to be around 300 μ m.

As part of the study the laser energy was varied within a wide range. One can suppose that there are no laser energy limitations for the plasma jet creation. For all laser energies from the range used in the experiment the very well formed plasma jet was produced. This opens possibility of the jet production and investigation at different-scale laser facilities.

The results reported in this paper have proved that the laser-produced plasma strongly modifies the initial distribution of the laser intensity. The outcome of this modification depends on both the position of the focal point, related to the target surface, and its distance from the target. Whereas the best jets can be formed at the beam spot radius $R_L(+)=250~\mu m$, if the focal point is located inside the target, for the opposite focal point position the optimum conditions for jets occur at $R_L(-)=400~\mu m$. In both these cases, the laser-produced craters have similar dimensions and shapes. On the contrary, at $R_L(-)=250~\mu m$ the laser intensity concentration is too strong, and at $R_L(+)=400~\mu m$ the laser radiation scattering too large for the jets to be produced.

Finally, we demonstrate one of possible applications of the plasma jet for investigations of different physical processes. The very simple method of supersonic plasma jets production in laboratory conditions, proposed here, constitutes a convenient tool in both the astrophysical and the inertial confinement fusion investigations.

Collaboration

Association EURATOM – IPP.CR, Prague, Czech Republic PALS Research Center, AS CR, Prague, Czech Republic Centre Lasers Intenses et Applications, Universite Bordeaux, Talence, France